



Habib, G., Bucciarelli-Ducci, C., Caforio, A. L. P., Cardim, N., Charron, P., Cosyns, B., Dehaene, A., Derumeaux, G., Donal, E., Dweck, M. R., Edvardsen, T., Erba, P. A., Ernande, L., Gaemperli, O., Galderisi, M., Grapsa, J., Jacquier, A., Klingel, K., Lancellotti, P. (2017). Multimodality Imaging in Restrictive Cardiomyopathies: An EACVI expert consensus document In collaboration with the "Working Group on myocardial and pericardial diseases" of the European Society of Cardiology Endorsed by The Indian Academy of Echocardiography. *European Heart Journal - Cardiovascular Imaging*, 18(10), 1090-1121. <https://doi.org/10.1093/ehjci/jex034>

Peer reviewed version

Link to published version (if available):  
[10.1093/ehjci/jex034](https://doi.org/10.1093/ehjci/jex034)

[Link to publication record in Explore Bristol Research](#)  
PDF-document

This is the accepted author manuscript (AAM). The final published version (version of record) is available online via OUP at <https://doi.org/10.1093/ehjci/jex034> . Please refer to any applicable terms of use of the publisher.

## University of Bristol - Explore Bristol Research

### General rights

This document is made available in accordance with publisher policies. Please cite only the published version using the reference above. Full terms of use are available: <http://www.bristol.ac.uk/red/research-policy/pure/user-guides/ebr-terms/>

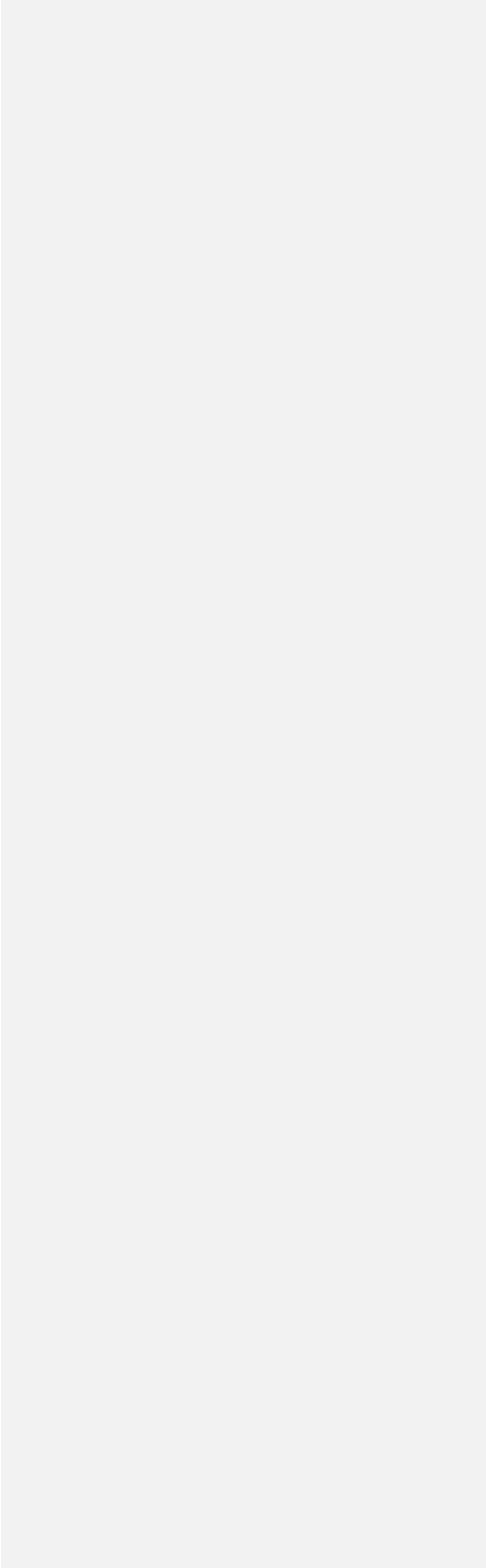
1  
2  
3  
4  
5  
6  
7  
8  
9  
10  
11  
12  
13  
14  
15  
16  
17  
18  
19  
20  
21  
22  
23  
24  
25  
26

**Multimodality Imaging  
in Restrictive Cardiomyopathies**

**An EACVI expert consensus document**

**In collaboration with  
the “Working Group on myocardial and pericardial diseases”  
of the European Society of Cardiology.**

**Endorsed by  
The Indian Academy of Echocardiography**



27

## Authors list

- 28 Gilbert HABIB 1 Aix- Marseille Univ, URMITE, Aix Marseille Université- UM63, CNRS 7278, IRD 198,  
29 INSERM 1095
- 30 2 APHM, La Timone Hospital, Cardiology Department, Marseille France
- 31 Chiara BUCCIARELLI-DUCCI Bristol Heart Institute Bristol NIHR Biomedical Research Unit (BRU) University  
32 of Bristol
- 33 Alida L. P. CAFORIO, MD, PhD, FESC, Cardiology, Department of Cardiological Thoracic and Vascular  
34 Sciences, University of Padova, Italy
- 35 Nuno CARDIM Multimodality cardiac imaging department, Sports Cardiology and cardiomyopathies centre-  
36 Hospital da Luz; Lisbon, Portugal
- 37 Philippe CHARRON 1 - Faculty hospital Ambroise Paré, 9 av Charles de Gaulle, 92104 Boulogne Billancourt -  
38 2 - Faculty hospital Pitié-Salpêtrière, 47 bvd de l'Hôpital, 75013 Paris, France
- 39
- 40 Bernard COSYNS MD, PhD. CHVZ (Centrum voor Hart en Vaatziekten - UZ Brussel
- 41 Aurélie DEHAENE APHM, Hôpitaux de la Timone, Pôle d'imagerie Médicale, Department of Radiology and  
42 Cardiovascular Imaging, 13005 Marseille, France
- 43 Genevieve DERUMEAUX INSERM U955, Université Paris-Est Creteil, Henri Mondor Hospital, DHU-ATVB,  
44 Department of Physiology, AP-HP, Créteil, France
- 45 Erwan DONAL Cardiologie – CHU Rennes & CIC-IT 1414 & LTSI INSERM 1099 – Université Rennes-1
- 46 Marc R Dweck: Centre for Cardiovascular Science, University of Edinburgh
- 47 Thor EDVARSDEN Department of Cardiology, Center for Cardiological innovation and Institute for 8 Surgical  
48 Research, Oslo University Hospital, Oslo Norway and University of 9 Oslo, Oslo, Norway
- 49 Paola Anna Erba MD, PhD. Department of Translational Research and New Technology in Medicine. University  
50 of Pisa. Pisa. Italy.
- 51 Laura ERNANDE INSERM U955, Université Paris-Est Creteil, Henri Mondor Hospital, DHU-ATVB, Department  
52 of Physiology, AP-HP, Créteil, France
- 53 Oliver GAEMPERLI University Heart Center Zurich, Interventional Cardiology and Cardiac Imaging 19 Zurich
- 54 Maurizio GALDERISI Department of Advanced Biomedical Sciences, Federico II University, Naples Italy
- 55 Julia GRAPSA Department of Cardiovascular Sciences, Imperial College of London, London, United Kingdom
- 56 Alexis JACQUIER APHM, Hôpitaux de la Timone, Pôle d'imagerie Médicale, Department of Radiology and  
57 Cardiovascular Imaging, Aix-Marseille Université, CNRS, CRMBM UMR 7339, 13385 Marseille, France
- 58 Karin KLINGEL Karin Klingel Department of Molecular Pathology, Institute for Pathology and Neuropathology,  
59 University Hospital Tuebingen, Tuebingen, Germany
- 60 Patrizio LANCELLOTTI 1. University of Liège Hospital, GIGA Cardiovascular Sciences, Departments of  
61 Cardiology, Heart Valve Clinic, CHU Sart Tilman, Liège, Belgium
- 62 2. Gruppo Villa Maria Care and Research, Anthea Hospital, Bari, Italy
- 63 Danilo NEGLIA Cardiovascular Department at Fondazione Toscana G. Monasterio, CNR Institute 32 of  
64 Clinical Physiology and Scuola Superiore San"Anna, Pisa, Italy.
- 65
- 66 Alessia PEPE MD, PhD, Magnetic Resonance Imaging Unit. Fondazione G. Monasterio C.N.R.- Regione Toscana  
67 Pisa, Italy
- 68 Pasquale PERRONE-FILARDI Department of Advanced Biomedical Sciences, Federico II University, Naples Italy

69 Steffen E. PETERSEN Department of Advanced Cardiovascular Imaging, William Harvey Research Institute,  
70 National Institute for Health Research Cardiovascular Biomedical Research Unit at Barts, London, United  
71 Kingdom

72 Sven PLEIN, MD, PhD, Multidisciplinary Cardiovascular Research Centre & Division of Biomedical Imaging,  
73 Leeds Institute of Cardiovascular and Metabolic Medicine LIGHT Laboratories, University of Leeds, United  
74 Kingdom

75 Bogdan A. Popescu University of Medicine and Pharmacy "Carol Davila" - Eurocolab, Institute of  
76 Cardiovascular Diseases, Bucharest, Romania

77 Patricia REANT, MD, PhD CHU de Bordeaux, Bordeaux, France

78 L. Elif SADE MD. Baskent University Ankara TURKEY

79 Erwan SALAUN La Timone Hospital, Cardiology Department, Marseille France

80 Riemer H.J.A. SLART <sup>1</sup>Department of Nuclear Medicine and Molecular Imaging, University of Groningen,  
81 University Medical Center Groningen, Hanzeplein 1, Groningen, The Netherlands

82 <sup>2</sup> Department of Biomedical Photonic Imaging, University of Twente, PO Box 217,  
83 7500 AE Enschede, The Netherlands

84 Christophe TRIBOUILLOY Department of Cardiology, University Hospital Amiens, Amiens, France and  
85 INSERM U-1088, Jules Verne University of Picardie, Amiens, France

86 Jose ZAMORANO University Hospital Ramon y Cajal Carretera de Colmenar Km 9,100 28034 Madrid. Spain

87

88

89

90

## 91 **Abstract**

92 Restrictive cardiomyopathies are a diverse group of myocardial diseases with a wide range  
93 of aetiologies, including familial, genetic and acquired diseases and ranging from very rare  
94 to relatively frequent cardiac disorders. In all these diseases, imaging techniques play a  
95 central role. Advanced imaging techniques provide important novel data on the diagnostic  
96 and prognostic assessment of restrictive cardiomyopathies. This EACVI consensus  
97 document provides comprehensive information for the appropriateness of all non-invasive  
98 imaging techniques for the diagnosis, prognostic evaluation, and management of patients  
99 with RCM.

100

101 **Key words:** echocardiography; cardiac magnetic resonance; computed tomography;  
102 nuclear imaging; cardiomyopathies; restrictive cardiomyopathies

103

104

# Table of Contents

105	
106	
107	<b>1. Introduction</b>
108	<b>2. Definition and classification of RCM</b>
109	<b>3. Pathophysiology of RCM and clinical presentation</b>
110	<b>4. Imaging modalities in RCM:</b>
111	1 - Echocardiography
112	2 - Cardiovascular magnetic resonance (CMR)
113	3 - Cardiac computed tomography (CT)
114	4 - Nuclear imaging
115	<b>5. Main forms of RCM and value of imaging techniques:</b>
116	<b>1 - Apparently idiopathic RCM</b>
117	<b>2 - Cardiac amyloidosis</b>
118	<b>3 - Other causes of familial/genetic RCM</b>
119	Hemochromatosis
120	Fabry cardiomyopathy
121	Glycogen storage disease
122	Pseudoxanthoma elasticum
123	<b>4 - Non familial/non-genetic RCM: Inflammatory cardiomyopathies with a restrictive</b>
124	<b>hemodynamic component:</b>
125	Cardiac Sarcoidosis
126	Systemic sclerosis
127	<b>5 - Non familial/non genetic RCM: Radiation therapy and cancer drug therapy induced RCM:</b>
128	Cardiac toxicity of radiation therapy
129	Cancer drug induced RCM
130	<b>6 - Endomyocardial RCMs</b>
131	Endomyocardial fibrosis
132	Hypereosinophilic syndrome
133	Carcinoid heart disease
134	Drug-induced endomyocardial fibrosis
135	
136	
137	<b>6. Differential diagnosis between RCM and other cardiac diseases</b>
138	Differential diagnosis between RCM and constrictive pericarditis
139	Differential diagnosis or association between RCM and other myocardial diseases
140	
141	<b>7. Conclusion and future directions</b>
142	

143 **1. Introduction**

144 Restrictive cardiomyopathies (RCM) are a diverse group of myocardial diseases with a wide  
145 range of aetiologies, including familial, genetic and acquired diseases and ranging from very  
146 rare to relatively frequent cardiac disorders. This diversity is also reflected in the  
147 inconsistent classification of RCM across guidelines (1-3) and even in the term “restrictive”,  
148 which is a functional characterization, unlike the morphological definition of the three other  
149 main types of cardiomyopathies, i.e. hypertrophic, arrhythmogenic right ventricular or  
150 dilated cardiomyopathies (4).

151 Independently of the underlying cause, the pathophysiology and clinical presentation, the  
152 initial phenotypic diagnosis of RCM requires imaging techniques. Many advances have  
153 occurred in the last decade in the diagnostic and prognostic assessment of RCM. This EACVI  
154 consensus document provides comprehensive information for the appropriateness of all  
155 non-invasive imaging techniques for the diagnosis, prognostic evaluation, and management  
156 of patients with RCM.

157 This article was written in close collaboration between the European Association of  
158 Cardiovascular Imaging (EACVI) and the Working Group (WG) on Myocardial and Pericardial  
159 diseases of the European Society of Cardiology (ESC). The types of RCM covered in this  
160 document are those included in the classification system proposed by the WG on Myocardial  
161 and Pericardial diseases (1) as well as some non-sarcomeric hypertrophic cardiomyopathies  
162 with a restrictive physiology that in previous classifications were included in the RCM  
163 category, e.g. cardiac amyloidosis.

164

165 **2. Definition and classification of RCM**

166 RCM is the least common type of the cardiomyopathies, defined as *myocardial disorders in*  
167 *which the heart muscle is structurally and functionally abnormal in the absence of coronary*  
168 *artery disease, arterial systemic hypertension, valvular disease or congenital heart disease*  
169 *sufficient to cause the observed myocardial abnormality* (1).

170 According to the historical World Health Organization (WHO) (2) and the updated definition  
171 proposed by the ESC WG on Myocardial and Pericardial Diseases in 2008 (1), each  
172 cardiomyopathy type is described by its clinical presentation. This approach is  
173 recommended firstly because it is the starting point in everyday clinical practice, and  
174 secondly because knowledge of aetiologies is still evolving, thus at present an aetiological  
175 classification would not be conclusive.

176 RCM is defined by restrictive ventricular physiology in the presence of normal or reduced  
177 diastolic volumes, with normal or near-normal left ventricular (LV) systolic function, and  
178 normal or near-normal wall thickness (1-5). Increased interstitial fibrosis may be present.  
179 RCM constitutes a heterogeneous group of heart muscle diseases with various causes (Table  
180 1) that may be classified according to very different criteria.

181 According to the main pathophysiological mechanism, RCM may be subclassified into  
182 infiltrative or storage diseases (e.g. amyloidosis and glycogen storage disease); obliterative  
183 or endomyocardial diseases (e.g. endomyocardial fibrosis, related or not to  
184 hypereosinophilia).

185 The WHO classification system was based on the distinction between primary and secondary  
186 myocardial disorders (2). Primary cardiomyopathies were defined as either not caused by an  
187 identifiable agent, e.g. idiopathic, or related to a primary myocardial cause. Secondary  
188 diseases were related to systemic disorders affecting the myocardium with a  
189 pathophysiological process starting outside of, e.g. unspecific to the myocardium. The  
190 American Heart Association (AHA) proposed a slightly different classification system in  
191 which the term “primary” was used to describe diseases in which the heart is the sole or  
192 predominantly involved organ whereas “secondary” is used to describe diseases in which  
193 myocardial dysfunction is part of a systemic disorder (3).

194 However, the challenge of distinguishing primary and secondary disorders is illustrated by  
195 the fact that many diseases classified as primary cardiomyopathies (e.g. glycogen storage  
196 disease, mitochondrial cytopathies) in the AHA classification can be associated with major  
197 extra-cardiac manifestations. Conversely, pathology in many of the diseases classified as  
198 secondary cardiomyopathies can predominantly (or exclusively) involve the heart (e.g.  
199 endomyocardial fibrosis or Fabry disease cardiac variant). In addition, the term of primary  
200 cardiomyopathy as an idiopathic condition is no longer appropriate in a large group of  
201 patients since genetics has identified mutations in various genes such as sarcomeric causes.  
202 Therefore, the ESC WG on Myocardial & Pericardial Diseases proposed in 2008 to abandon  
203 the distinction between primary and secondary causes (1).

204 As an alternative to this classification, the ESC Working Group on Myocardial and  
205 Pericardial Diseases proposed to subclassify RCM and other cardiomyopathies into (i)  
206 familial or genetic causes and (ii) non-familial/non-genetic causes, because of the recent  
207 and increasing knowledge about genetic causes of cardiomyopathies. This is especially  
208 illustrated in RCM related to cardiac amyloidosis that may be acquired (amyloidosis AL or  
209 senile amyloidosis) or genetically determined (transthyretin and other genes mutations) and

210 be included in the nonsarcomeric hypertrophic cardiomyopathies as well as in the RCM (1).  
211 The latter ESC classification will be used in this position paper.

212

### 213 **3. Pathophysiology of RCM and clinical presentation**

214 Restrictive physiology is characterized by a pattern of LV filling in which increased stiffness  
215 of the myocardium causes a precipitous rise of LV pressure with only small increases in  
216 volume. On cardiac catheterization, this phenomenon is characterized by a dip-and-plateau  
217 contour of early diastolic pressure traces. The standard echocardiographic features of  
218 'restrictive' filling are described in chapter 4.1

219 Similarly, Some patients with a restrictive physiology may have significantly increased wall  
220 thickness such as patients with cardiac amyloidosis. RCM should be differentiated from  
221 constrictive pericarditis (6, 7). (see chapter 5).

222

### 223 **4. Imaging modalities in RCM:**

#### 224 **1 - Echocardiography**

225 Echocardiography plays a key role for the recognition of RCM. The echocardiographic  
226 diagnosis requires to differentiate RCM from constrictive pericarditis.

227 RCM are usually characterized by normal or small LV cavity size ( $< 40\text{mL}/\text{m}^2$ ) with preserved  
228 LV ejection fraction, bi-atrial enlargement, and diastolic dysfunction (5).

229 Assessment of LV diastolic function and filling pressures is of utmost value in RCM. In the  
230 recent joint American Society of Echocardiography (ASE) / EACVI recommendations for the  
231 evaluation of diastolic function by echocardiography (8), the four recommended variables to  
232 diagnose LV diastolic dysfunction and their abnormal cut-off values are annular e' velocity  
233 (septal e'  $< 7$  cm/s, lateral e'  $< 10$  cm/s), average E/e' ratio  $> 14$ , LA maximum volume index  
234  $> 34$  ml/m<sup>2</sup>, and peak TR velocity  $> 2.8$  m/s (figure 1). Other valuable parameters to identify  
235 the presence of elevated LV filling pressures are the ratio of pulmonary vein peak systolic to  
236 peak diastolic velocity, or systolic time velocity integral to diastolic time velocity integral  $< 1$ ,  
237 and the changes in E/A ratio with Valsalva manoeuvre. The restrictive filling is considered  
238 reversible if the change of E/A ratio during Valsalva is  $\geq 0.5$  and fixed if it is  $< 0.5$  (more  
239 severe form).

240 The diagnosis of RCM does not equal the presence of restrictive physiology. Patients with  
241 true RCM may present with a grade I diastolic dysfunction and move progressively to grade



242 II or III diastolic dysfunction, with worsening of their disease. The advanced stages of RCM  
243 are characterized by typical restrictive physiology with a mitral inflow E/A ratio > 2.5, DT  
244 of E velocity <150 ms, IVRT < 50 ms, decreased septal and lateral e' velocities ( 3-4 cm/s),  
245 E/e' ratio > 14, as well as a markedly increased LA volume index (> 50 ml/m<sup>2</sup>)(8), this  
246 advanced restrictive pattern being associated with the worst prognosis (9). Wall thickness  
247 is usually normal.

Commented [v1]: Try to avoid grades of LV diastolic dysfunction since they have not been introduced earlier

Commented [GH2R1]: Ok deleted

248 Some specific features may also help differentiate secondary RCM, including several  
249 systemic conditions (diabetic cardiomyopathy, scleroderma, endomyocardial fibrosis,  
250 radiation, chemotherapy, carcinoid heart disease, metastatic cancers), from apparently  
251 idiopathic RCM (see chapter 5). Ultrasonic tissue characterisation with integrated  
252 backscatter has been used to assess myocardial texture, but is non-specific (10, 11). Finally,  
253 2D deformation imaging is useful for the assessment of LV longitudinal dysfunction, which  
254 is frequently impaired in most forms of RCM (12) (see chapter 5), and may help  
255 differentiating RCM from constrictive pericarditis (13)

Commented [v3]: This sentence cannot come now because you have not indicated the differences between RCM and constrictive pericarditis

Commented [GH4R3]: Ok deleted

256

## 257 **2 - Cardiovascular magnetic resonance (CMR)**

258 CMR imaging can contribute importantly to the diagnosis of RCM and the differential  
259 diagnosis from pericardial constriction [14]. The CMR methods most commonly used for the  
260 assessment of RCM include static (black blood) images, cine and contrast enhanced imaging  
261 as well as parametric mapping.

262 Static images are used to delineate cardiac, pericardial and vascular morphology. T1 and  
263 T2 weighted black blood images are sensitive to different tissue characteristics and provide  
264 complementary information. T1 weighted images show high signal from fat, as may for  
265 example be seen in Fabry's disease, while T2 weighted short tau inversion recovery (STIR)  
266 images show high signal in myocardial oedema, for example in acute sarcoidosis.

267 CMR allows accurate volumetric assessment of the heart and can accurately measure  
268 chamber size and function [15]. Typical cine CMR images are averaged over several heart  
269 beats to maximize image quality and temporal resolution, but real-time imaging can also be  
270 performed to demonstrate the typical septal shift during respiratory maneuvers and identify  
271 restrictive physiology [16]. Velocity encoded CMR in standardized imaging planes  
272 perpendicular to the atrio-ventricular heart valves is used to demonstrate the typical  
273 restrictive filling patterns of accentuated early filling and absent or reduced late filling [17].

Commented [v5]: This I agree that is an important sentence. But this is not specific for RCM. It is for every single cardiac disease. The word count should be kept <10,000 words. Please try to keep the sentences that are relevant for this specific topic.

Commented [GH6R5]: Ok deleted

274 A unique feature of CMR of relevance to the imaging of RCM is tissue characterization with  
275 late gadolinium enhancement (LGE). Following intravenous administration gadolinium  
276 based contrast agents are retained preferentially in tissues with an expanded extracellular  
277 space, such as fibrosis, scar or infiltration. Characteristic patterns of contrast enhancement  
278 can be observed in several of the RCMs, contributing to the differential diagnosis of Fabry  
279 disease, amyloidosis, endomyocardial fibrosis and sarcoidosis (Figure 2). In many of these  
280 conditions, the presence of LGE also has important prognostic relevance [18-20]. Finally,  
281 parametric mapping methods have increasing applications in RCM and allow quantitative  
282 measurement of tissue characteristics. T2\*-weighted CMR is now the method of choice to  
283 detect and quantify myocardial iron content in iron deposition cardiomyopathy and to guide  
284 appropriate therapy [21]. A low myocardial T2\* value in this context is currently considered  
285 the most powerful marker of adverse outcome [22]. More recently, T1 mapping has been  
286 used to quantify the extent of myocardial inflammation and fibrosis. Native T1 relaxation  
287 times, as measured with T1 mapping without the need for contrast agent administration,  
288 are altered in several conditions including amyloidosis and may have incremental value over  
289 LGE imaging [23]. The combination of native and post contrast T1 mapping allows an  
290 estimation of the myocardial extracellular volume (ECV) fraction, which in amyloidosis can  
291 even show differences in subtypes of the disease [24]. T1 mapping may also be useful in  
292 iron overload instead of the more established T2\* mapping [25].

293

Commented [v7]: This is good for a book chapter. But this is repetitive of what is said before. Please consider deleting it.

Commented [GH8R7]: Ok deleted

### 294 **3 - Cardiac computed tomography (CT)**

295 The key advantage of computed tomography (CT) is its high-spatial resolution and the  
296 anatomical detail it provides. However the associated radiation exposure largely limits this  
297 modality to static imaging, precluding dynamic analyses of left ventricular haemodynamics,  
298 filling or relaxation. Nevertheless CT is well suited to identifying the anatomic features of  
299 impaired cardiac filling that characterize RCM. These include dilatation of the atria,  
300 coronary sinus and inferior vena cava and the presence of pulmonary congestion and pleural  
301 effusions. These features are also observed in a range of other conditions and the  
302 predominant role of CT with respect to RCM is in the exclusion of these alternative  
303 diagnoses. In particular, CT is well suited to detecting the thickening and calcification of  
304 the pericardium most commonly associated with constrictive pericarditis (26). Similarly CT  
305 allows assessment of extra-cardiac involvement in systemic conditions such as sarcoidosis  
306 (e.g. pulmonary nodules, pulmonary fibrosis and lymphadenopathy) or amyloidosis (e.g.  
307 inhomogeneous hepatomegaly, diffuse lung parenchymal involvement, small kidneys)  
308 further aiding in the differential diagnosis.

309 When other imaging modalities are not available, CT may be useful in evaluation of patients  
310 with RCM, owing to its ability to measure LV wall thickness and mass, detect regional wall  
311 thickening (27), regions of replacement fibrosis (27, 28), and measure myocardial  
312 extracellular volume fraction by equilibrium contrast-enhanced CT to assess diffuse fibrosis  
313 (29). These advances may increase the clinical utility of CT in the future clinical assessment  
314 of patients with RCM, particularly when echocardiography and CMR are non-diagnostic or  
315 contraindicated.

316

#### 317 **4 – Nuclear imaging**

318 Nuclear imaging modalities have a potential clinical role in two forms of RCM: amyloidosis  
319 and sarcoidosis (see chapters 5.2 and 5.4). Nuclear imaging modalities have the advantage  
320 of specific targeted molecular imaging. Positron emission tomography (PET) has the  
321 technical advantages of high spatial resolution, robust built-in attenuation correction,  
322 quantitative analysis, and low patient radiation exposure, whereas single photon emission  
323 computed tomography (SPECT) has the advantage of a robust, cheaper and well validated  
324 camera system

325 There are increasing data on the role of nuclear tracers with SPECT and more recently with  
326 PET for early identification and differential diagnosis of cardiac amyloidosis, particularly  
327 transthyretin-related amyloidosis (ATTR)

328 Radiolabelled SPECT phosphate derivatives, initially developed as bone-seeking tracers,  
329 were noted to localize to amyloid deposits using [99mTc]-diphosphanate (30). In clinical  
330 practice, the most used SPECT tracers are: 99mTc-DPD mainly in Europe and Asia and  
331 99mTc-PYP in the United States. Their main advantage is avid uptake by **ATTR** and minimal  
332 uptake with the light-chain (AL) amyloidosis subtype, providing one of the best non-invasive  
333 ways to differentiate these subtypes of cardiac amyloidosis. (31, 32)

334 The imaging technique is simple. Briefly, after administering 740 MBq of 99mTc-DPD, or or  
335 [99mTc]-HDP (32, 33), or of 99mTc-PYP (34) intravenously, a whole-body scan is performed  
336 3 hours or 1 h later (anterior and posterior projections). If there is active uptake in the heart,  
337 chest SPECT is performed. The analysis is performed by semi-quantitative visual scoring of  
338 the cardiac as compared to the bone uptake (scores from 0 to 3) and by computing the ratio,  
339 after correction for background counts, of the mean counts in the heart region over the  
340 mean counts in the contralateral chest ( H/CL ratio).

Commented [v9]: abbreviation

Commented [GH10R9]: ok abbreviation above

341 Other nuclear imaging approaches have been recently proposed for the diagnosis and  
342 prognostic stratification of patients with suspected amyloidosis. (31) PET imaging using new  
343 amyloid tracers like the [11C]-labeled Pittsburgh Compound B (PiB) or [18F]-florbetapir is  
344 promising and under early clinical investigation. The use of neuronal imaging by [123-I]-  
345 MIBG SPECT has been suggested for early recognition of cardiac involvement and prognostic  
346 stratification of individuals with TTR mutation (34)

347 The inflammatory nature of cardiac sarcoidosis renders PET useful for its diagnosis, as  
348 [<sup>18</sup>F]FDG accumulates in inflammatory cells in the heart. FDG is preferred in combination  
349 with a perfusion tracer to improve specificity, due to better match/mismatch pattern  
350 recognition. Unlike in CMR, there is no distinct pattern of FDG uptake that is  
351 pathognomonic for cardiac sarcoidosis, though focal or focal on diffuse uptake is suggestive  
352 of the disorder.(35) At present, [<sup>18</sup>F]FDG-PET appears to be more sensitive but less specific  
353 than CMR (36) and its use seems most appropriate in patients who have contraindications  
354 to CMR, inconclusive findings on CMR or where CMR is not available also to monitor  
355 response to therapy. The development of FDG PET/MR techniques offers the ability to  
356 assess LV wall function, the pattern of myocardial injury and disease activity in a single  
357 scan (37) (figure 3 )

358

359 *In summary, several imaging techniques are available in the evaluation of RCM, all of which*  
360 *have both advantages and limitations. Table 2 summarizes the value of different imaging*  
361 *modalities in various forms of RCM. Although non-invasive techniques are sufficient in most*  
362 *cases, final histologic diagnosis may sometimes be necessary, and may be obtained by*  
363 *biopsies specimens from the heart (endomyocardial biopsies [EMB]) or other organs. Figure 4*  
364 *illustrates by histology and immunohistology different disease entities of RCM which will be*  
365 *discussed in the following chapters.*

366

367

368

369

370

**Commented [v11]:** this is not really addressed in these sections...it goes a bit against the value of the imaging techniques. Delete it ?

**Commented [GH12R11]:** I agree. However, histologic description was requested by the majority and difficult to withdraw this part. It was really a wish from the Cardiomyopathy WG to include this sentence, which has already been shortened previously. I tried to introduce some nuances in the role of histology, which may be sometimes useful, and widely used in some countries

371 **5. Main forms of RCM and value of imaging techniques:**

372 **1 – Apparently idiopathic RCM**

373 Apparently idiopathic RCM may be caused by mutations in sarcomeric disease genes and  
374 may even coexist with hypertrophic cardiomyopathy in the same family (38-40) and may  
375 require EMB (to exclude cardiac amyloidosis), family screening and genetic investigations.  
376 Most affected individuals have severe signs and symptoms of heart failure. Several studies  
377 have reported that 66–100% die or receive a cardiac transplant within a few years of  
378 diagnosis.

379 The echocardiographic diagnosis is one of restrictive physiology and mostly preserved LV  
380 ejection fraction. Typically, idiopathic RCM is characterised by diastolic dysfunction with  
381 apparently preserved systolic function, dilated atria, and the absence of ventricular  
382 hypertrophy or dilatation (figure 5 and videos 1 and 2). Longitudinal function may be  
383 decreased; the right ventricle may be involved but there is no “pathognomonic”  
384 echocardiographic pattern of apparently idiopathic RCM. CMR with LGE may facilitate the  
385 diagnosis of infiltrative myocardial disease, and is thus particularly useful for ruling out a  
386 particular cause of RCM (41).

387

388 **2 – Cardiac amyloidosis**

389 Cardiac amyloidosis (CA) is one of the most frequent causes of RCM and may be  
390 genetic/familial (ATTR) or non-genetic non-familial (AL/ prealbumin, senile). | |

391 The diagnosis requires awareness, expertise and a high level of clinical suspicion, with  
392 integration between clinical, electrocardiographic and echocardiographic data. The  
393 “mismatch” between the presence of LV hypertrophy (LVH) in echocardiography and its  
394 absence on the ECG (no LVH, absolute or relative low-voltage QRS) is suggestive of cardiac  
395 amyloidosis and is often the first disease “red flag” (42, 43). Typical echocardiographic  
396 findings in cardiac amyloidosis patients include (figure 6a) a non-dilated LV with moderate  
397 concentric LVH and a ‘granular sparkling’ appearance of the myocardial texture, valvular  
398 thickening (mainly the A-V valves), biatrial dilatation, right ventricular free wall  
399 hypertrophy, inter atrial septum infiltration (loss of physiological echo drop-out) and mild  
400 pericardial effusion (44). In the early stages of the disease, cardiac amyloidosis may present  
401 as asymmetrical septal hypertrophy, sometimes with LV outflow tract obstruction and can  
402 then be wrongly diagnosed as hypertrophic cardiomyopathy (HCM). The presence of intra-

Commented [v13]: this sentence does not provide much since the review is on imaging...

Commented [GH14R13]: ok

Commented [v15]: echocardiography is the first line for all RCM

Commented [GH16R15]: true

403 atrial thrombus also seems to be relatively frequent in patients with cardiac amyloidosis,  
404 even in sinus rhythm (45).

405 Patients often show (figure 6b) advanced diastolic dysfunction (grade II or III) and increased  
406 LV filling pressures. The classical transmitral restrictive pattern may only be seen at  
407 advanced disease stages. The typical tissue Doppler imaging (TDI) pattern of cardiac  
408 amyloidosis, with low systolic ( $s'$ ) and diastolic ( $e'$ ,  $a'$ ) myocardial velocities. Of note,  $E/e'$   
409 ratio is usually abnormally increased even in the presence of LV abnormal relaxation pattern  
410 (diastolic dysfunction grade I) (46).

411 LV systolic dysfunction is also a common finding in this disease. In early stages, despite  
412 preserved LV ejection fraction, longitudinal function is abnormal (abnormal long axis  
413 systolic velocities ( $s'$ ) and strain) (figure 7a) as well as myocardial contraction fraction, a  
414 recently described systolic parameter (47).

415 2D speckle-tracing echocardiography (2D-STE) is important, as many systolic strain  
416 parameters (longitudinal, circumferential, radial) are abnormal in cardiac amyloidosis,  
417 particularly in the longitudinal axis, typically with prominent involvement of LV basal  
418 segments and apical sparing (48) (figure 7b), reflecting the predominant deposition of  
419 amyloid in basal segments. The combination of a prominent reduction of longitudinal strain  
420 in LV basal segments with increased  $E/e'$  ratio suggests cardiac amyloidosis in early stages  
421 (49).

422 Multiple echocardiographic parameters have been associated with adverse outcomes in  
423 cardiac amyloidosis, including M- mode and 2D data (maximal wall thickness, LV fractional  
424 shortening and LV ejection fraction, right ventricle dilatation), blood pool Doppler data  
425 (restrictive filling pattern, myocardial performance index, Tissue Doppler derived data  
426 (myocardial velocities, long axis velocity gradient, peak longitudinal systolic basal antero-  
427 septal strain  $> -7.5\%$ ) (50) and 2D-STE parameters (GLS, mid-septum systolic longitudinal  
428 strain, apical LS  $< -14.5\%$ ) (51, 52).

429 CMR is often used after CA is suspected by echocardiography to confirm or refute the  
430 diagnosis, and in experienced hands represents a powerful tool with important diagnostic  
431 and prognostic implications. Cine images may demonstrate typical anatomical features like  
432 thickened LV wall, biatrial enlargement, reduced long-axis shortening, and pleural or  
433 pericardial effusion. The presence of amyloid protein in the myocardial interstitium is  
434 associated with abnormal gadolinium-chelate contrast kinetics and characteristic patterns  
435 of contrast distribution. LGE images typically show circumferential subendocardial contrast  
436 enhancement or bilateral septal subendocardial LGE with dark mid-wall (zebra pattern)

Commented [v17]: Lv diastolic function is abnormal in all RCM by definition ?

Commented [GH18R17]: yes

Commented [v19]: This sentence is repetition of the section on CMR. Please avoid repetition.

Commented [GH20R19]: ok

437 (Figure 8a) (53, 54), but other patterns of enhancement have also been described. In atypical  
438 cases, other differential diagnoses should be considered such as hypertrophic  
439 cardiomyopathy or Fabry's disease. Cardiac involvement can extend to the right ventricle  
440 and atrial walls, as potentially detected by LGE. The extent of myocardial LGE correlates  
441 with New York Heart Association functional class, LV wall thickness, lower ECG voltage,  
442 and cardiac biomarkers (troponins, brain natriuretic peptide)(55). With more advanced  
443 disease, amyloid infiltration may be transmural with corresponding global enhancement on  
444 LGE images, which is an independent predictor of poorer outcomes, over stroke volume and  
445 pro-NT brain natriuretic peptide. (56)

446 Amyloid deposits increase the longitudinal relaxation time (T1) magnetic property of  
447 the heart. Thus, myocardial non-contrast T1 values are longer in cardiac amyloidosis than  
448 in controls, a finding with higher sensitivity for detecting early subclinical cardiac  
449 involvement than LGE.(57) ECV estimation from pre- and post-contrast T1 mapping has  
450 been used to quantify interstitial amyloid deposition which appears to be more extensive in  
451 transthyretin amyloidosis (TTR) than in immunoglobulin light-chain amyloidosis (AL). (58)  
452 The addition of parametric mapping to standard CMR images is promising to be a powerful  
453 and quantitative diagnostic tool that also allows differential diagnosis from other diseases  
454 with similar phenotypic expression.

455 Scintigraphy employs molecular-targeted radiolabeled compounds to detect systemic and  
456 organ-specific amyloid deposits. Scintigraphy is a valuable alternative to CMR particularly  
457 for patients with ATTR amyloidosis due to its very high sensitivity. Scintigraphy may also  
458 be used following an inconclusive CMR study, or for phenotyping cardiac amyloidosis (ATTR  
459 vs. AL) or in the differential diagnosis with sarcomeric HCM (59, 60). ). The [99mTc]-labeled  
460 bisphosphonate compounds pyrophosphate (PYP) (60) and 3,3-diphosphono-1,2-  
461 propanodicarboxylic acid (DPD)(61) and hydroxydiphosphonate (HDP) (33) (which are  
462 routinely used as bone scintigraphy agents) bind through unknown mechanisms to amyloid  
463 protein. All have proven very sensitive for detecting cardiac involvement in ATTR amyloidosis  
464 with reported sensitivities up to 100% on late phase planar scintigraphy. Typical uptake  
465 patterns besides cardiac uptake in ATTR amyloidosis include increased soft tissue uptake  
466 (mainly muscular uptake in the gluteal, shoulder, chest and abdominal wall regions) with  
467 obscuring of bone uptake (Figure 8b). However, in AL amyloidosis, cardiac uptake is found  
468 in less than half of patients and is generally less intense (likely due to the lower  
469 concentration of calcium-containing products in AL amyloid). Additionally, AL patients have  
470 generally no muscular [99mTc]-DPD or [99mTc]-HDP uptake while visceral uptake (liver,  
471 spleen) may be more common.

472 Even if there are not yet large comparative studies, the diagnostic performance of  
473 nuclear imaging for cardiac amyloidosis is established. In general, [99mTc]-DPD can  
474 differentiate subtypes (62) and can be more sensitive than CMR (33) or echocardiography in  
475 diagnosing early disease being an independent prognostic marker (63). In a recent study by  
476 Bokhari et al. (60) using 99mTc-PYP, while patients with AL had some uptake, the visual  
477 score was significantly less than in patients with ATTR, allowing the differentiation between  
478 ATTR and AL amyloidosis with 97% sensitivity and 100% specificity.

479 Hence, whole body planar DPD and HDP scintigraphy may help to phenotype cardiac  
480 amyloidosis particularly through differentiating ATTR from AL amyloidosis (or from  
481 sarcomeric HCM, where no DPD uptake is seen), which often have overlapping imaging  
482 features on echocardiography and CMR, but very distinct clinical course and prognosis.  
483 Moreover, a recent comparison of [99mTc]-DPD scintigraphy and LGE showed that despite  
484 a general good agreement between both techniques, LGE may sometimes underestimate  
485 cardiac amyloid burden (33). Finally, myocardial tracer uptake on scintigraphy is correlated  
486 with disease severity (measured by circulating troponin and LV wall mass), and has been  
487 shown to be a powerful prognostic determinant of outcome in ATTR cardiac amyloidosis (32,  
488 63).

489 Recent investigations found that bone scintigraphy enables the diagnosis of cardiac ATTR  
490 amyloidosis to be made reliably without the need for histology in patients who do not have  
491 a monoclonal gammopathy. (64). The algorithm proposed (figure 9) that cardiac ATTR  
492 amyloidosis can be reliably diagnosed in the absence of histology provided an  
493 echocardiogram or CMR is suggestive of amyloidosis, cardiac uptake is present on  
494 scintigraphy and there is absence of a detectable monoclonal gammopathy. Histological  
495 confirmation and typing of amyloid should be sought in all cases of suspected cardiac  
496 amyloidosis in which these criteria are not met.

497 ***In summary, all these imaging techniques are useful and give additional***  
498 ***information, including echocardiography, nuclear techniques, CMR (table 3 (65), but***  
499 ***also EMB and genetic testing, to differentiate ATTR mutant from wild type. Figure***  
500 ***10 illustrates the value of multimodality imaging in a patient with cardiac***  
501 ***amyloidosis.***

502

503

504

Commented [v21]: Said before ?

Commented [v22]: If these sections are meant to be like keypoints, this sentence can be deleted



505 **3 – Other causes of familial/genetic RCM**

506 **Hemochromatosis**

507 Iron overload cardiomyopathy (IOC) results from iron accumulation in the myocardium  
508 mainly because of genetic disorders of iron metabolism (primary hemochromatosis) or  
509 multiple transfusions (such as in thalassemia or myelodysplastic syndromes).

510 In the early stages, myocardial iron overload (MIO) causes diastolic LV dysfunction (66). If  
511 no effective iron chelation is instituted in time, the majority of patients develops LV  
512 dilatation and reduced LV ejection fraction (EF) (dilated phenotype) (67). In a minority of  
513 cases with severe MIO, restrictive LV dysfunction can lead to pulmonary hypertension, right  
514 ventricular dilatation, and right-sided heart failure with preserved LVEF (restrictive  
515 phenotype) (68).

516 Echocardiography is a useful modality in the follow-up of iron-loaded patients. A  
517 pseudonormalized pattern of transmitral inflow is frequently encountered and may be  
518 unmasked by tissue Doppler (69). LV diastolic dysfunction and reduced EF may both be  
519 masked by an anemia-induced high cardiac output state in hematologic patients. There are  
520 few data relating diastolic function to outcome in hemochromatosis (70).

521 However, due to the lower accuracy in quantifying biventricular systolic function and the  
522 lack of parameters able to predict MIO reliably, echocardiography is only the second-line  
523 imaging method after CMR (71, 72).

524 The method of choice for assessing IOC is CMR, which allows tissue characterization  
525 including quantification of MIO. The paramagnetic effect of iron-loaded myocardium affects  
526 T1, T2 and T2\* relaxation times which can be used to calculate MIO. The best validated  
527 method for quantifying MIO is T2\* mapping. T2\* values correlate closely with hepatic and  
528 myocardial iron content and correlate better with LV dilatation and LV dysfunction than  
529 serum ferritin or liver iron concentration. A T2\* value of < 20 ms at 1.5 Tesla, typically  
530 measured in the interventricular septum, is used as a conservative cut-off for segmental  
531 and global heart iron overload and patients with the lowest T2\* values have the highest risk  
532 of developing arrhythmia and heart failure. T2\* CMR has revolutionized IOC management  
533 with the death rate in patients with Thalassemia falling dramatically in countries where T2\*  
534 CMR has been adopted. In the assessment of IOC, the first cardiac T2\* assessment should  
535 be performed as early as possible and the effectiveness of iron chelation (73) and reversal of  
536 MIO can be reliably guided by follow up scans (74). A multislice approach can detect the  
537 uneven distribution of MIO, allowing early identification of patients at risk of cardiac  
538 complications (75).

**Commented [v23]:** This is known worldwide. Please avoid information that is already known and not specific of this disease.

**Commented [v24]:** If not enough data, try to avoid it...

**Commented [v25]:** This we know it is common for every single cardiac disease. Please indicate the most important features that make any imaging technique unique for specific disease...

539 T2\* is dependent on field strength and sensitive to field inhomogeneity. T2 and T1 mapping  
540 techniques offer some advantages over T2\* and have been compared with standard methods,  
541 with initial studies showing close correlation with T2\*.

542 In patients where the diagnosis is unclear, a multiparametric CMR approach that evaluates  
543 cardiac function, myocardial fibrosis and edema may allow further clarification of the  
544 underlying mechanisms leading to the LV dysfunction (76).

545  
546 *In summary, cardiac involvement is frequent in hemochromatosis. CMR is the main*  
547 *imaging technique for diagnosis and follow-up of cardiac hemochromatosis,*  
548 *allowing both reliable measurement of LV and RV dimension and function and tissue*  
549 *characterization including quantification of MIO.*

550

### 551 **Fabry cardiomyopathy**

552 Cardiac involvement is very common and is the most frequent cause of death not only in  
553 hemizygote males but also in female heterozygote carriers with  $\alpha$ -Gal A deficiency, with a  
554 reduction of life expectancy of approximately 20 and 15 years respectively (77). The heart  
555 may be the only organ affected in the classic phenotype of Fabry disease, and this is  
556 designated the “cardiac variant” (78).

557 Cardiovascular manifestations include renovascular and systemic hypertension, aortic root  
558 dilatation, mitral prolapse and congestive heart failure (79). Fabry cardiomyopathy mainly  
559 consists of progressive LVH, which may cause substantial morbidity and contribute to the  
560 reduced life expectancy of affected patients, both male and female (80, 81).

561 LVH is a hallmark of Fabry cardiomyopathy (82). In patient populations with HCM, the  
562 prevalence of Fabry disease ranges from 0 to 12%, depending on the patient selection criteria  
563 used, but is close to 1% in the largest series (83). LVH is generally symmetrical, although  
564 asymmetric septal hypertrophy has been described, and the condition can mimic the  
565 phenotypical and clinical features of HCM, including obstructive HCM (84). Typically, the  
566 echocardiogram shows marked increases in wall thickness and ventricular dilatation later  
567 in the disease process. Valve leaflet thickening can be seen, and this produces valve  
568 impairment that usually does not require surgical treatment (85).

569 Echocardiography using TDI can detect the first signs of myocardial damage in a patient  
570 with Fabry cardiomyopathy and normal cardiac wall thickness (86). Furthermore, TDI  
571 studies have been shown to be useful in detecting cardiac involvement in female carriers

572 with no systemic manifestations of Fabry disease. A reduction of TDI velocities may  
573 represent the first sign of initial intrinsic myocardial impairment (87). These reduced TDI  
574 velocities in mutation positives without LVH are consistent with the hypothesis that  
575 myocardial dysfunction precedes LVH (88).

576 CMR with LGE may be useful in the non-invasive recognition of myocardial fibrosis, in the  
577 context of cardiac involvement of Fabry disease (89). The LGE pattern of distribution helps  
578 in the differentiation between HCM and Fabry cardiomyopathy (90). Patients with Fabry  
579 cardiomyopathy typically present with a pattern characterized by the involvement of the  
580 inferolateral basal or mid basal segments (89). Furthermore, the myocardial T2 relaxation  
581 time is prolonged in patients with Fabry disease compared with that in HCM patients, and  
582 its measurement could be complementary to the LGE technique. More recently, native T1  
583 mapping was shown to be the most reliable technique to differentiate Fabry cardiomyopathy  
584 from all the other LVH phenocopies, by demonstrating a low native T1 value of the affected  
585 myocardium (whilst other LGE area of different disease would display a high native T1  
586 values) (90). This important difference is due to the characteristic fatty nature of the  
587 infiltration in Fabry disease.

588 Finally, for most males with Fabry disease, the diagnosis can be made by measuring  
589 leucocyte and plasma  $\alpha$ -Gal activity, while genetic testing is useful in patients with normal  
590 levels of enzyme activity (90). A familial screening should be performed in patients with  
591 Fabry's disease (figure 11).

592  
593 ***In summary, cardiac involvement is frequent in Fabry disease and is associated with***  
594 ***worse outcome. Imaging techniques, especially TDI and CMR, allow a comprehensive***  
595 ***evaluation of cardiac involvement, even before morphological manifestations such***  
596 ***as hypertrophy develop.***

597  
598 **Glycogen storage disease**

599 Glycogen storage disease is defined as the absence or deficiency of one of the enzymes  
600 responsible for making or breaking down glycogen in the body. The enzyme deficiency  
601 causes either abnormal tissue concentrations of glycogen or incorrectly or abnormally  
602 formed glycogen (91, 92). There are 11 different types of glycogen storage diseases causing  
603 different forms of heart failure. Most well-known are Danon and Pompe diseases (82, 93,  
604 94).

605 Danon cardiomyopathy is progressive and typically manifests a hypertrophic phenotype,  
606 with preserved LVEF and normal cavity dimensions early in the course of disease, and later  
607 progression to dilated features in 11% to 12% of men (92). Hypertrophic cardiomyopathy is  
608 predominant in male patients, whereas an equal prevalence of hypertrophic and dilated  
609 cardiomyopathy is seen in female patients (93).

Commented [v26]: Really needed for an imaging article ?

610 Echocardiography demonstrates increased LV mass and wall thickness although LV systolic  
611 function is preserved. Taking into consideration the possible progress to cardiac failure,  
612 serial echocardiograms with attention to LV thickness and mass are important in the care  
613 of these patients (94, 95). Echocardiography is also the standard method to evaluate the  
614 cardiac response to enzyme replacement therapy.

Commented [v27]: Already said before ?

615 Typical findings in CMR consist of significantly reduced LV global function and increase of  
616 LV end-diastolic and end-systolic volumes. Perfusion defects, mainly subendocardial, are  
617 visible in almost all segments on rest first-pass perfusion images. They may be obvious in  
618 the infero-septal segments and partly transmural in the lateral and anterior walls. LGE  
619 appears to be a rare finding in Pompe disease but when present, is seen in the  
620 subendocardium and in places transmurally in the anterior and lateral walls (96, 97).

621 A diagnosis of Danon disease is always confirmed by EMB results.

622 <sup>99m</sup>Tc-methoxyisobutylisonitrile (MIBI) myocardial imaging has also been employed as an  
623 imaging diagnostic test for glycogen storage disease, to detect myocardial damage as a non-  
624 invasive method. There has been a positive rate of detection of damage with G-MPI of 77.8  
625 % (98).

626 Other storage / infiltrative diseases (Gaucher disease, mucopolysaccharidoses) may be  
627 rarely associated with cardiac involvement (99, 100).

628

629

### 630 **Pseudoxanthoma elasticum**

631 Pseudoxanthoma elasticum is a rare, inherited connective tissue disorder associated with  
632 coronary and peripheral arterial disease and accelerated atherosclerosis in medium sized  
633 arteries (101). Cardiac involvement may start as a diffuse arteriopathy secondary to elastic  
634 fiber dysgenesis, involving the small intramural coronary vessels ('small-vessel disease') and  
635 it may reach the clinical presentation of congestive heart failure, even though – quite often  
636 – with normal epicardial vessels (102).

637 Echocardiography detects impaired LV systolic and diastolic function (103). Other imaging  
638 modalities – as functional tests – such as perfusion CMR or nuclear myocardial perfusion  
639 imaging, may be useful to demonstrate early coronary involvement and/or the direct

640 consequences of ultrastructural defects of the elastic tissue of the heart. Increased  
641 awareness for silent ischemia is recommended (101, 104).

642 An important study with arterial stiffness evaluation demonstrates the early detection of  
643 accelerated atherosclerosis and the impairment of the elastic properties of the aorta. A lower  
644 elasticity in large arteries, a higher cardiac output and a higher total vascular impedance  
645 were observed in patients with pseudoxanthoma elasticum with respect to the control group  
646 (104).

647

648

#### 649 **4 - Non familial/non-genetic RCM: Inflammatory cardiomyopathies** 650 **with a restrictive hemodynamic component:**

##### 651 **Cardiac Sarcoidosis**

652 Sarcoidosis is a multisystem inflammatory granulomatous disease of unknown origin.  
653 Cardiac sarcoidosis (CS) is frequently isolated (105). Its diagnosis is difficult and has  
654 benefited from the use of multimodality imaging.

655 Although echocardiography is not the method of choice for the diagnosis of cardiac  
656 sarcoidosis, it can offer very useful information in some cases (106). An unexplained reduced  
657 LV ejection fraction <40% in a patient with a histological diagnosis of extra-cardiac  
658 sarcoidosis is suggestive of cardiac sarcoidosis (107). Characteristic echocardiographic  
659 changes suggestive of cardiac sarcoidosis are: wall thickness >13 mm (due to  
660 granulomatous expansion), or <7 mm (due to fibrosis), aneurysmal dilatation especially at  
661 the level of the inferior and posterior walls (108), regional wall motion abnormalities without  
662 any specific coronary distribution, interspersed with normokinetic segments (109).

663 CMR is one of the imaging modalities recommended for the diagnosis of cardiac sarcoidosis  
664 in current guidelines (106) and CMR may be more sensitive for cardiac involvement than  
665 currently used clinical criteria (110). Myocardial inflammation may be identified by T2 STIR  
666 images and early contrast enhancement while areas of fibrosis are detected by LGE (111)  
667 (figure 12). The typical pattern of cardiac sarcoidosis on LGE is patchy focal enhancement  
668 sparing the endocardial border, not following a coronary artery distribution (112), and  
669 involving mainly the basal and lateral LV walls (113). Single or often multiple lesions are  
670 seen and other, more atypical LGE patterns have also been described. Importantly, no LGE  
671 pattern is pathognomonic for CS. Moreover, CMR offers prognostic information: myocardial  
672 scar determined by LGE is a predictor for ventricular arrhythmia and sudden cardiac death  
673 in patients with sarcoidosis (114).

674 Nuclear imaging has also an important role in the assessment of cardiac sarcoidosis.  
675 Although the major diagnostic criteria for CS include [67Ga]-citrate scintigraphy, its  
676 sensitivity for CS is significantly lower than [18F]FDG-PET/CT (115). For this reason  
677 [18F]FDG-PET/CT have currently replaced [67Ga]-scintigraphy in the majority of centers  
678 being nowadays the most commonly used imaging test for detecting myocardial  
679 inflammation. Advantages of [18F]FDG-PET/CT over [67Ga], includes favorable tracer  
680 kinetics, lower radiation exposure, and better quality images (116). Active sarcoid lesions  
681 present increased [18F]FDG uptake on PET/CT imaging due to utilization of glucose as an  
682 energy source by inflammatory cell in infiltrates (117). However, [18F]FDG-PET/CT has not  
683 been officially adopted in the diagnostic guidelines (118) mainly due to the high variability  
684 of [18F]FDG uptake in the normal myocardium, that requires adequate patient preparation  
685 to prevent errors. Strategies for myocardial suppression to maximize the accuracy of the  
686 procedure include prolonged fasting, dietary modifications, and a heparin load before  
687 imaging (119). The imaging protocol include preferable gated cardiac [18F]FDG and whole  
688 body images (120). A cardiac perfusion scan could be combined to compare [18F]FDG-PET  
689 and perfusion patterns (Table 4) (121).

690 Pitfalls in [18F]FDG PET/CT imaging are myocarditis, cardiac amyloidosis, infection, and  
691 myocardial metastases, causing focal [18F]FDG uptake. There are very few circumstances  
692 under which [18F]FDG will be falsely negative as in case of corticosteroids treatment or “old,  
693 non-active” sarcoidosis.

694 [18F]FDG-PET/CT sensitivity and specificity for CS have been reported at 89% and 78%,  
695 respectively (117). Quantitative analysis further improved these figures, reaching a  
696 sensitivity of 97.3% and a specificity of 83.6% for the diagnosis of CS. In addition,  
697 standardized uptake value (SUVmax) on [18F]FDG-PET/CT was found the only independent  
698 predictor among clinical and imaging variables for diagnosing CS (122) .

699 Serial [18F]FDG-PET/CT imaging can be utilized to assess the response to therapies.  
700 Decrease [18F]FDG uptake in cardiac lesions following therapy has been reported in case of  
701 corticosteroid treatment as well as immunosuppressive therapies (123, 124). **Figure 13**  
702 illustrates the value of serial [18F]FDG PET/CT in a patient with CS treated with high dose  
703 corticosteroids.

704 [18F]FDG-PET/CT only moderately correlated with CMR, mainly due to the different  
705 significance of findings: LGE by CMR represents cardiac damage and scarring whereas  
706 [18F]FDG uptake represents active inflammation. When CMR and [18F]FDG -PET/CT were  
707 compared with the Japanese Ministry of Health and Welfare guidelines (JMHWG), CMR had  
708 a higher specificity with lower sensitivity than nuclear imaging (125) .

709

710 **In summary, [18F]FDG-PET/CT and CMR are powerful imaging techniques for accurate**  
711 **detection and therapy monitoring of CS. Protocols for imaging with these modalities**  
712 **are increasingly well defined, however large prospective studies supporting new**  
713 **guidelines for CS imaging are warranted.**

714

### 715 **Systemic sclerosis**

716 Systemic sclerosis (SSc) is a connective tissue disease characterized by vascular and fibrotic  
717 lesions of skin and internal organs and represents a model of progressive interstitial  
718 myocardial fibrosis triggered by increased endothelin production and also focal  
719 hypoperfusion (126). Cardiovascular involvement has been shown to be one of the leading  
720 causes of mortality in SSc and can occur in up to 70% of patients as a finding on autopsy  
721 (127, 128). Although the primary myocardial involvement remains clinically silent in the  
722 majority of patients, it can lead to further diastolic and systolic LV dysfunction (129), which  
723 carries a poor prognosis. Early diagnosis and accurate staging of myocardial involvement  
724 are therefore crucial for the management of these patients and for therapeutic strategies.

725 Conventional echocardiographic assessment of the LVEF has shown limited sensitivity being  
726 able to identify only 5% of patients with cardiac involvement (130). Results of studies using  
727 TDI and speckle-tracking echocardiography suggested that myocardial velocity and strain  
728 might be more sensitive than conventional measures in identifying subtle cardiac  
729 dysfunction in asymptomatic patients with SSc (131, 132).

730 Since myocardial fibrosis is the primary abnormality underlying SSc cardiac involvement,  
731 methods that enable early identification of fibrosis should be preferred. Endomyocardial  
732 biopsy is the gold standard for the detection of myocarditis that may be found in SSc  
733 patients and might help to detect cardiac involvement at an early stage of the disease as  
734 inflammation was found in 96 % and fibrosis in 100% of all SSc patients investigated (133).  
735 Importantly, prognosis was poor and associated with the degree of cardiac inflammation  
736 and fibrosis revealing an event rate of 28% within 22.5 months follow-up (133).

737 CMR with LGE imaging has been used to detect myocardial areas with replacement fibrosis  
738 in patients with an advanced stage of SSc (134). However, at an early stage of the disease,  
739 myocardial fibrosis in SSc is usually diffuse and thus, undetected by LGE-CMR. ECV  
740 estimation using pre and post contrast T1 mapping has been used to visualize increased  
741 collagen content in SSc (135). A recent study has demonstrated that ECV imaging performed  
742 early during SS reveals myocardial abnormalities consistent with diffuse myocardial fibrosis  
743 that are not apparent on LGE imaging, therefore representing an early marker of disease.  
744 (136). In addition, the ECV abnormalities correlated with diastolic LV dysfunction which

745 occurred in 45% of the patients (137). This study also evaluated the systolic circumferential  
746 strain by CMR that was also found decreased but without any correlation with ECV increase,  
747 suggesting therefore that LV systolic dysfunction may be related not only to myocardial  
748 fibrosis but also to other phenomena, such as myocardial ischemia.

749 In SSc, myocardial ischemia, unrelated to coronary artery disease, is common with  
750 impairment of microcirculation and coronary vasospasm (138). Therefore, stress  
751 echocardiography, CMR stress perfusion and single-photon emission computed tomography  
752 (SPECT) have been proposed to evaluate myocardial perfusion in SS patients

753

754

## 755 **5 - Non familial/non genetic RCM: Radiation therapy and cancer** 756 **drug therapy induced RCM:**

### 757 **Cardiac toxicity of radiation therapy**

758 In general, the development of radiotherapy-induced RCM suggests a prior high dose chest  
759 irradiation (>60 Gy). It can also occur at lower radiation exposure when anthracycline is  
760 used (139). RCM occurs as a result of diffuse myocardial fibrosis. On echocardiography, the  
761 classical features of RCM are found. Although its value in radiation-related myocardial  
762 fibrosis is still unclear, ECV estimation using pre and post contract T1 mapping by CMR is  
763 directly related to collagen content (140). The presence of decreased mean LV mass, end-  
764 diastolic dimension, and end-diastolic wall thickness together with dilation of both atria and  
765 self-reported dyspnea, is suggestive of RCM in this population (141). Cardiac CT has little  
766 value in the diagnosis of RCM after radiotherapy, except for the detection of any associated  
767 vascular disease. There is no proven value of nuclear cardiology in the detection of RCM  
768 after radiation exposure. However, perfusion scintigraphy imaging can reveal fixed regional  
769 perfusion defects, which possibly indicate direct damage and the presence of local fibrosis  
770 (142).

771

772

### 773 **Cancer drug induced RCM**

774 The typical structural manifestation of cancer drug induced cardiomyopathy corresponds  
775 to a LV eccentric remodeling with dilation of internal cavity and thinning of myocardial walls  
776 [143]. When clinical heart failure is overt, this picture is associated with a significant  
777 reduction of LV ejection fraction. In the more advanced stages LV diastolic function can be  
778 strongly altered, with an abnormal increase of LV filling pressure. This will induce the  
779 classic "restrictive" physiology with the typical standard Doppler-derived transmitral

**Commented [v28]:** Is this specific for this type of RCM ? from previous description this is common to all of them ?



780 pattern: E/A ratio > 2 or even > 3 and short E velocity deceleration time (usually < 150-160  
781 msec). The presence of a restrictive pattern in a patient with cancer drug induced  
782 cardiotoxicity has a recognized prognostic value, exactly as this occurs in the general clinical  
783 setting [8].

784 Currently, the restrictive diastolic pattern is detectable in particular in patients undergoing  
785 anthracyclines (Cardiotoxicity type 1), it being possibly evident not only during treatment  
786 (acute cardiotoxicity) but also - and more often - after the completion (even several years  
787 after) of cancer therapies [143]. (figure 14, videos 6 and 7). Early cardiotoxicity, occurring  
788 during or within 1 year of completion of treatment, is the most important risk factor for the  
789 development of late cardiotoxicity, which occurs beyond a year of completion of treatment.  
790 This is very important to know in children undergoing anthracyclines therapy. In fact, they  
791 can develop late cardiotoxicity during adulthood and should be therefore carefully  
792 monitored for years by echocardiography. Cumulative as well as peak anthracycline doses  
793 affect adults and children alike.

794 The restrictive physiology of diastolic pattern is instead very rare in patients undergoing  
795 trastuzumab therapy and similar drugs (Cardiotoxicity type 2) [143]. This kind of  
796 cardiotoxicity is usually reversible with cancer therapy interruption. However, since  
797 trastuzumab can be sequentially added to anthracyclines, a combined effect anthracyclines  
798 + trastuzumab on the degree of LV filling pressures cannot be excluded and should therefore  
799 be carefully monitored.

800 When a restrictive LV diastolic pattern is detectable in patients receiving cancer drugs, the  
801 echocardiographic exam should be extended to a quantitative evaluation of LV longitudinal  
802 function. In fact, when high levels of LV filling pressure are evident, a reduction of global  
803 longitudinal strain (GLS), measurable by speckle tracking echocardiography, is usually  
804 observed. If speckle tracking echocardiography is not available, pulsed tissue Doppler  
805 derived s' velocity of the mitral annulus or even the simple M-mode derived mitral annular  
806 plane systolic excursion represent much more than simple surrogates of LV longitudinal  
807 dysfunction.

808 In this cohort of patients, CMR can be useful both for the accurate volumetric assessment  
809 with cine imaging but also with the LGE technique for the detection of myocardial fibrosis  
810 [143], i.e., the first determinant of LV diastolic dysfunction and LV filling pressure increase.

811  
812  
813  
814  
815

**Commented [v29]:** This is also the same than everywhere. It should be kept to highlight the points characteristic for each RCM type.

816 **6 – Endomyocardial RCMs**

817 **Endomyocardial fibrosis**

818 Endomyocardial fibrosis (EMF) is an often-neglected disorder in the tropical and subtropical  
819 regions of the world which is characterized by the development of a restrictive  
820 cardiomyopathy (144), and is associated with a high morbidity and mortality (145). As  
821 etiologic causes of endomyocardial fibrosis, infections, inflammation, allergy, malnutrition  
822 and toxic agents are discussed (146). At the histological level, EMF is characterized by a  
823 marked endocardial thickening due to the deposition of fibrous tissue (Figure 15)(147).

824 An echocardiographic examination of 1063 individuals revealed that most subjects (55%)  
825 had a biventricular involvement, and 28% revealed a right-sided prevalence with mild-  
826 moderate structural and functional echocardiographic abnormalities (148).

827 Regarding the diagnosis of EMF, transthoracic echocardiographic changes can be useful for  
828 visualizing structural abnormalities, especially in chronic EMF (145, 147). The main  
829 echocardiographic features include apical obliteration of the left and / or right ventricles,  
830 reduced volume of the ventricular cavity, endocardial thickening and a restrictive pattern.  
831 (figure 16, video 8)

832 Endomyocardial fibrosis may be difficult to differentiate from other cardiomyopathies  
833 (Loeffler's endocarditis, Churg-Strauss syndrome or rheumatoid arthritis, tuberculous  
834 pericarditis, constrictive pericarditis or apical HCM (145, 149-151). After initial  
835 echocardiographic analysis, CMR (152) including LGE imaging should be performed which  
836 is now the gold standard for imaging the disease.(figure 17) In a CMR study of 36 patients  
837 it was shown that LGE-CMR can provide detailed information on ventricular morphology,  
838 including the existence of thrombus or calcifications, and revealing functional information  
839 which is useful in the diagnosis and prognosis of EMF through quantification of the typical  
840 pattern of the endocardial fibrous tissue deposition (153). Adjunctive diagnostic tools, such  
841 as EMB, can be considered in ambiguous cases (154) and can help in patient management.

842

843

844 **Hyper eosinophilic syndrome**

845 Eosinophilic endomyocardial fibrosis is a rare cause of RCM, resulting from toxicity of  
846 eosinophils towards cardiac tissues (155). The causes for eosinophilic infiltration of  
847 myocardium are hypersensitivity, parasitic infestation, systemic disease, myeloproliferative  
848 syndrome and idiopathic hyper eosinophilic syndrome (155).

849 Cardiac disease follows three stages, with involvement of the endocardium, the myocardium  
850 and the pericardium. The first is eosinophilic myocarditis (acute necrotic stage) due to

851 infiltration of eosinophils and release of the contents of their granules in the myocardium  
852 (155). There is no relationship between the extent of the infiltrate and clinical symptoms  
853 (156). The intermediate phase is the thrombotic stage, characterized by mural thrombi along  
854 the damaged endocardium (more often in the apex of the left ventricle). The third stage is  
855 the later fibrotic stage in which the granulation tissue is changed into hyaline fibrosis. The  
856 endocardial scar can result in a decrease of ventricular compliance and in RCM (157).  
857 On echocardiography, classical findings are progressive endomyocardial thickening, apical  
858 obliteration of one or both ventricles by echogenic material suggestive of fibrosis or  
859 thrombus formation, posterior mitral leaflet involvement and papillary dysfunction resulting  
860 in mitral regurgitation (157, 158) (figure 18a). Pericardial effusion can be present as well as  
861 the typical RCM pattern of normal-to-small ventricles with large atria (159).  
862 Echocardiography can also be useful for monitoring the effects of specific therapies on the  
863 reversal of endomyocardial infiltration in hypereosinophilic cardiomyopathy (160).  
864 CMR is very useful in endomyocardial fibrosis, both for diagnosis of endocardial involvement  
865 and for detection of thrombus formation in both ventricles (161-164)(figure 18b). The gold  
866 standard is EMB but the high resolution of CMR and TTE is frequently sufficient for  
867 diagnosis and follow-up. (3).

868

869

### 870 **Carcinoid heart disease**

871 Carcinoid heart disease occurs in 20% to 70% of patients with metastatic carcinoid tumors  
872 and will lead to increased morbidity and mortality in these patients. (165) The endocardial  
873 fibrosis results in retraction and fixation of the heart valves. Right-sided valves are mainly  
874 affected(166). Left-sided valvular pathology occurs in approximately 10% of patients with  
875 carcinoid heart disease and is associated with right-to-left shunting, bronchial carcinoid, or  
876 poorly controlled carcinoid syndrome. (167, 168).

877 The hallmarks of carcinoid heart disease are a combination of right-sided valvular  
878 dysfunction and typical morphological changes of the valves like valve leaflet thickening,  
879 shortening, retraction, reduced mobility, or incomplete coaptation of the tricuspid leaflets.  
880 (169- 171). CMR has an additive value in carcinoid heart diseases, especially when  
881 echocardiography is inconclusive and for accurate measurements of right ventricular  
882 function and assessment of carcinoid plaques using LGE (171). Figure 19, videos 9 and 10,  
883 illustrate the value of multimodality imaging in a patient with carcinoid heart disease.

884

885

**Commented [v30]:** all this is not related per se to the RCM physiology. Please indicate the typical findings that make the diagnosis of RCM. The valves is another story.

886 **Drug-induced endomyocardial fibrosis**

887 Animal data suggest the possibility of drug-induced endomyocardial fibrosis induced by 5-  
888 HT2B serotonin receptor agonists such as fenfluramine derivatives, pergolide, cabergolide  
889 and methysergid and ergotamine (172-174), but very scarce data are currently reported in  
890 man. Indeed, only one case of RCM is reported after fenfluramine-phentermine exposure  
891 (175). In addition, a case of sub-aortic obstruction within the LV outflow tract related to  
892 drug-induced endomyocardial fibrosis has been recently reported in a patient exposed to  
893 benfluorex, an agonist of 5-HT2B serotonergic receptors (176).

**Commented [GH31]:** This chapter was again shortened but it should be kept since is part of the classification of RCM given by the cardiomyopathies WG

894 |  
895

**Commented [v32]:** If only 1 case has been reported showing RCM, I would delete this section

896 **6. Differential diagnosis between RCM and other cardiac diseases**

897 **Differential diagnosis between RCM and constrictive pericarditis**

898 Differential diagnosis between RCM and constrictive pericarditis (CP) can be a challenge as  
899 their clinical presentation is relatively similar with right heart failure symptoms, preserved  
900 LV ejection fraction, and diastolic dysfunction. However, as the treatment of these two  
901 conditions is very different, constriction being potentially curable by surgery, making the  
902 correct diagnosis is critically important. The differential diagnosis could be performed  
903 particularly using the complementary elements obtained from TTE, CMR, cardiac CT, or  
904 cardiac catheterization. (table 5)

905 Cardiac catheterization was the first method historically used to help in the differential  
906 diagnosis of RCM and CP, but is not always conclusive (177, 178).

907 In both RCM and CP, biatrial dilatation, venous dilatation as well as pericardial effusion can  
908 be observed. Several echocardiographic parameters have been identified to differentiate  
909 myocardial diseases from pericardial constriction (10, 179). In case of RCM, some degree of  
910 LV or biventricular hypertrophy or unusual echo texture can be noted (RCM of infiltrative  
911 origin). In case of constrictive pericarditis, pericardial thickening (>3mm) or  
912 hyperechogenicity of the pericardium can be observed. But one of the main characteristics  
913 of CP is the absence of transmission of the intrathoracic pressure variations to the heart,  
914 which are physiologically present during the respiratory cycle.

**Commented [v33]:** abbreviation

**Commented [GH34R33]:** ok

915 Both TTE and real time cine CMR allow the identification of some key findings which  
916 differentiate the two pathologies: septal bulging occurring with cavity volume variations and  
917 the exaggerated respiratory-related LV-RV coupling highlighted by a respiratory septal shift  
918 observed in CP and a significant respiratory variation of the diastolic flow. The respiratory  
919 septal shift is defined by a difference in the maximal septal excursion into LV between

920 inspiration and expiration (Video 11).(179) Using CMR, this parameter has a sensitivity of  
921 80% and specificity of 100% to detect CP. (180)

922 Other echocardiographic findings have been reported to be useful for differentiating RCM  
923 and CP, including TDI (e'), E velocity deceleration time, pulmonary vein flow, left atrial  
924 volume, and E/e' ratio (181). Figure 20 shows an algorithm proposed by the recent ASE /  
925 EACVI recommendations for the evaluation of diastolic function by echocardiography (8),  
926 comparing constrictive pericarditis and RCM. The presence of a normal annular e' velocity  
927 in a patient referred with heart failure diagnosis should raise suspicion of pericardial  
928 constriction (8).

929 LV myocardial velocities (182-185) and deformation (11) measured by both TTE and CMR  
930 (186) are reduced at a greater degree in RCM compared to constrictive pericarditis. Both  
931 echocardiography and CMR provide concordant diagnostic information and incremental  
932 value for differentiating constrictive pericarditis from RCM. Complementary assessment of  
933 structural (pericardial thickening), mechanical (myocardial velocities and strains) and  
934 hemodynamic (respiratory septal shift) by both TTE and CMR and their complementary use  
935 increase the cost-efficacy and confidence for the diagnosis of RCM vs. constrictive  
936 pericarditis.

937 Cardiac CT provides excellent anatomic delineation of the pericardium, allowing for accurate  
938 measurement of pericardial thickness (abnormal if >4mm) (187), although a normal  
939 pericardial thickness does not exclude constrictive pericarditis (188). Cardiac CT is superior  
940 to CMR in detecting pericardial calcifications (189). Finally, multimodality imaging should  
941 be performed in patients with suspected constrictive pericarditis, since each imaging  
942 modality presents with both advantages and limitations (table 5, figure 21)

943  
944 ***In summary, the differentiation between RCM and constrictive pericarditis is***  
945 ***frequently difficult and should take into account both clinical presentation and***  
946 ***multimodality imaging. The absence of pericardial thickening does not rule out***  
947 ***constrictive pericarditis. Echocardiography, CMR and CT provide complementary***  
948 ***information and in many patients all three should be performed when constrictive***  
949 ***pericarditis is suspected.***

950  
951

952 **Differential diagnosis or association between RCM and other**  
953 **myocardial diseases**

954 Although in its most typical « apparently idiopathic » form, RCM presents without LV  
955 hypertrophy, in some patients, some forms of cardiomyopathy may resemble or be  
956 associated with RCM. Particularly, HCM may resemble RCM in some patients. The classical  
957 HCM phenotype presents with enhanced contractility, small cavity, reduced indexed stroke  
958 volume, LVOT obstruction, grade 1 diastolic dysfunction with some fibrosis (190, 191). As  
959 the disease progresses, extensive fibrosis (52), reduced systolic function (52), diastolic  
960 dysfunction (192, 193), marked dilatation of the atria (194), relative thinning of the LV walls,  
961 loss of LVOT obstruction (194-196) and pulmonary hypertension (196) dominate the picture,  
962 mimicking RCM.

963 Isolated LV non-compaction is a rare form of cardiomyopathy (197), which should also be  
964 differentiated from RCM, but is also sometimes associated with a restrictive pattern or even  
965 a true RCM (198) (figure 22, video 12)

966

967

968 **7. Conclusion and future directions**

969 RCM represents a heterogeneous group of cardiac diseases, with different  
970 pathophysiological processes, clinical presentation, treatment, and prognosis. The two main  
971 objectives of the clinician are to rule out constrictive pericarditis, and to find a potentially  
972 treatable cause of RCM. Imaging techniques including echocardiography, cardiac CT, CMR,  
973 and nuclear techniques are of utmost value for the diagnostic and prognostic assessment  
974 of RCM. These techniques give additional information and should frequently be used in  
975 combination in the same patient to maximize diagnostic performance. Finally, additional  
976 investigations such as endomyocardial biopsy, familial screening, and genetic studies are  
977 frequently necessary in these patients. For these reasons, patients with suspected RCM  
978 should be referred to specialized centers that can provide multimodality imaging and a  
979 multidisciplinary team approach.

980

981

982

983

**Commented [v35]:** this sentence kills a bit the entire purpose of the review because it seems that there is no consensus on which imaging technique we have to use first. Honestly, in 99% of cases the patient will get an echo first (even before doing the anamnesis).

984

985

986 **Figure legends:**

987

988 Figure 1: ASE – EACVI criteria for grading LV diastolic function in patients with depressed LVEF and  
989 patients with myocardial disease and normal LVEF after consideration of clinical and other 2D data.  
990 (from reference 8 with permission)

991

992 Figure 2: 74 year old patient presenting with breathlessness. Cine CMR showed global left ventricular  
993 hypertrophy, impaired longitudinal LV shortening and dilated atria. Late gadolinium enhanced CMR  
994 in the figure showed diffuse endocardial enhancement consistent with infiltrative disease.  
995 Subsequently the patient was found to have amyloidosis. LV: left ventricle; RV: right ventricle; LA:  
996 left atrium; RA: right atrium

997

998 Figure 3: Patient With Acute Myocardial Sarcoidosis (from reference 37 with permission)  
999 Patient (62-year-old male) followed for histologically proven pulmonary sarcoidosis treated by steroids  
1000 for 10 years presented with symptoms of acute breathlessness. Cardiac involvement was suspected.  
1001 LGE-CMR (A) images showed patchy LGE of the lateral wall. Matched FDG-PET (B) and fused FDG-  
1002 PET/MR (C and D) images obtained in short-axis view showed intense uptake in exactly the same  
1003 territory as the pattern of injury on CMR (maximum standardized uptake value of LGE territory/blood  
1004 pool uptake ratio = 2.7). A 2-chamber cine CMR (E) sequence showed mild hypokinesis of the lateral  
1005 wall and mild overall left ventricular systolic impairment (left ventricular ejection fraction = 52%).  
1006 Maximum intensity projection FDG-PET (F) cine view confirmed abnormal myocardial uptake without  
1007 evidence of increased activity outside of the heart.

1008

1009 Figure 4: Imaging of RCM at the cellular level. Different disease entities of RCM are visualized by  
1010 histology and immunohistology. Sarcoidosis with typical granulomas, fibrosis (blue tissue) (A,  
1011 Masson trichrome stain) and numerous CD68+ macrophages and giant cells (B,  
1012 immunohistochemistry). Hypereosinophilic syndrome with myocyte necrosis, eosinophilic  
1013 granulocytes (C, Giemsa stain) and CD68+macrophages (D, immunohistochemistry). Storage  
1014 diseases: Hemochromatosis with iron containing myocytes (E, Prussian blue), and fibrosis (F, Sirius  
1015 red). AL-amyloidosis (G, AL-amyloid immunohistochemistry (green), H, Kongo red). Glycogenosis with  
1016 hypertrophic, vacuolated myocytes and fibrosis (I, Masson trichrome stain) and large amounts of  
1017 glycogen (J, PAS stain (red)). (A,B x 100x, C-J x200).

1018

1019

1020 Figure 5: echo findings in 3 patients with apparently idiopathic RCM.

1021 5a and video 1(TTE), 5b (CMR): impressive dilatation of both atria predominating on the right  
1022 cavities, contrasting with small LV and RV cavities

1023 5c and video 2: more classical form of idiopathic RCM with normal ventricular systolic function and  
1024 severe atrial dilatation

1025 RA: right atrium, RV: right ventricle, LV: left ventricle, LA: left atrium

1026 5d: Multimodality imaging in a severe RCM. Patient in atrial fibrillation, and a pace maker for  
1027 severe atrio-ventricular block. Huge atria that can be seen on the CT (1), the chest X-ray (2) and  
1028 the Echocardiography (6). There is a severe tricuspid regurgitation (5) and a severe alteration of the  
1029 longitudinal systolic and diastolic function as shown by the tissue Doppler (5),and the strain data  
1030 (4). Extensive circumferential subendocardial late gadolinium enhancement is observed by CMR (3).

1031

1032 Figure 6a- 2D echocardiography in a 52 year-old male with cardiac amyloidosis, AL type, associated  
1033 with plasma cell dyscrasia: non- dilated LV with moderate concentric LVH with 'granular sparkling'  
1034 appearance, mitral valve thickening, mild to moderate biatrial dilatation, inter atrial septum  
1035 infiltration (loss of physiological echo drop-out) and mild pericardial effusion

1036 RA: right atrium, RV: right ventricle, LV: left ventricle, LA: left atrium, Ao: aorta

1037 Figure 6b- Diastolic function in the same patient: E/A >>1 (PWD transmitral inflow), low systolic  
1038 and diastolic myocardial velocities (TDI), E/e' =25, reflecting high LV filling pressures

1039

1040 Figure 7a- 2D-STE apical longitudinal view in systemic AL amyloidosis : severely abnormal  
1041 longitudinal strain, particularly in the basal and medial LV segments

1042 Figure 7b- Systemic AL amyloidosis , multiple myeloma: 2D-STE : Relative apical sparing, typical of  
1043 cardiac amyloidosis. Note the abnormal GLS ( -4,9%)

1044

1045 Figure 8a. CMR in a 79-year old patient with cardiac amyloidosis showing mild septal hypertrophy  
1046 (16mm), biatrial enlargement, and diffuse patchy uptake of gadolinium throughout the  
1047 midventricular and basal segments of the septal, anterior and inferior wall with sparing of the  
1048 apicolateral wall. (Note small areas of bilateral subendocardial LGE in the septal wall characteristic  
1049 of cardiac amyloidosis (arrows) and LGE in the right ventricular free wall and the left atrium).

1050 RA: right atrium, RV: right ventricle, LV: left ventricle, LA: left atrium

1051



1052 Figure 8b. Late-phase planar <sup>99m</sup>Tc-DPD-scintigraphy (anterior views) in a patient with ATTR  
1053 amyloidosis (A) and a normal control (B). Note intense cardiac uptake in (A) demonstrating cardiac  
1054 amyloidosis. Moreover, increased soft tissue uptake particularly in the shoulder region and the  
1055 abdominal wall with obscuring of bone uptake can be observed as a typical pattern of ATTR  
1056 amyloidosis.

1057  
1058 Figure 9: Diagnostic algorithm for patients with suspected amyloid cardiomyopathy. (from reference  
1059 64 with permission). AApoA1 indicates apolipoprotein A-I; DPD, 3,3-diphosphono-1,2-  
1060 propanodicarboxylic acid; HDMP, hydroxymethylene diphosphonate; and PYP, pyrophosphate.

1061  
1062 Figure 10: multimodality imaging in a patient with familial TTR amyloidosis  
1063 10a: and video 3: 2D echo long-axis view showing LV hypertrophy and pericardial effusion  
1064 10b: and video 4: apical sparing by 2D strain  
1065 10c: intense cardiac uptake on <sup>99m</sup>Tc scintigraphy  
1066 10d and video 5: CMR confirming LV hypertrophy and pericardial effusion  
1067 RV: right ventricle, LV: left ventricle, LA: left atrium, Per: pericardial effusion  
1068

1069 Figure 11: familial Fabry's disease in 2 brothers  
1070 - 11a: EKG in a 55 year-old male showing a pattern of apical hypertrophy  
1071 - 11b: apical transthoracic view showing an apical hypertrophy (arrow)  
1072 - 11c: CMR finding of predominantly apical hypertrophy  
1073 - 11d: inferolateral late gadolinium enhancement  
1074 - 11e: EKG in his young brother showing milder but similar abnormalities  
1075 - 11f: concentric diffuse hypertrophy in the brother  
1076 RV: right ventricle, LV: left ventricle, LA: left atrium, RA: right atrium  
1077

1078 Figure 12: Patient with known cardiac sarcoidosis. The image shows a late gadolinium enhanced  
1079 CMR image in the vertical long axis plane. Several focal areas of myocardial enhancement can be  
1080 seen (arrows) consistent with granulomatous myocardial infiltration.

1081  
1082 Figure 13: 41 year-old male with a total AV-block, bradycardia and weakness. The patient was  
1083 suspected of cardiac sarcoidosis. Echocardiography was normal. A FDG PET/CT was performed after  
1084 careful patient preparation with a fatty diet and showed heterogeneous, spotty high uptake in the  
1085 left ventricle of the heart (left whole body PET and upper row right short axis PET/CT). The patient  
1086 was treated with high dose corticosteroids and the repeated FDG PET/CT after 3 months shows fully  
1087 normalization of the myocardium (right whole body FDG PET/CT and lower short axis PET/CT).

1088  
1089  
1090

1091 Figure 14 and videos 6 and 7: 25 year-old woman treated for Hodgkin disease in infancy with  
1092 anthracyclins.

1093 Chest X ray (1) and echocardiography (2 and 3) show a non-dilated left ventricle, with a relatively  
1094 preserved LV contractility (video 6). However, mitral flow (4) and pulmonary venous flow (5) show a  
1095 severely restrictive pattern and tricuspid flow recording (6) reveals pulmonary hypertension. Severe  
1096 longitudinal dysfunction is evidenced by 2D strain (video 7)

1097

1098

1099 Figure 15: histologic finding in a patient with endomyocardial fibrosis

1100

1101

1102 Figure 16a and video 8 (TTE), 16b (CMR): right ventricular endomyocardial fibrosis in a 50 year-old  
1103 woman. The apex of the right ventricle is obliterated (white arrow), with subsequent surgical  
1104 confirmation.

1105 RA: right atrium, RV: right ventricle, LV: left ventricle, LA: left atrium

1106

1107 Figure 17: LV endomyocardial fibrosis in a 58 year-old man presenting with congestive heart failure

1108 17a: Cine 4 chamber view in end-diastolic phase showing a thickening of LV apex (black arrow), a  
1109 reduced volume of the left ventricular cavity and a left atrial enlargement.

1110 17b: LGE 4 chambers view showing a marked endocardial thickening with late gadolinium  
1111 enhancement (black arrow) and an apical thrombus (open arrow).

1112

1113

1114 Figure 18a: Multimodality imaging in hypereosinophilic syndrome with cardiac involvement showing  
1115 severe restriction of the posterior mitral leaflet associated with involvement of the subvalvular  
1116 apparatus and severe mitral regurgitation by echocardiography (a, b) and CMR (c) with worsening in  
1117 the follow-up (d). From reference 158 with permission

1118 RA: right atrium, RV: right ventricle, LV: left ventricle, LA: left atrium

1119

1120 Figure 18b: CMR in a patient with hypereosinophilic syndrome and Loeffler's syndrome. Cine image  
1121 (still frame) (A) demonstrates a dilated left ventricle and moderate pericardial effusion (asterisks).

1122 T2-weighted image (B,C) shows subendocardial high signal intensity suggestive of inflammation  
1123 (white arrows), and T1-weighted images after contrast administration (D-F) demonstrate

1124 endocardial fibrosis (arrowheads). Of note, an RV apical thrombus is evident in the cine image and  
1125 in the T1-weighted sequences (triangles) (from reference 162 with permission)

1126

1127 Figure 19, videos 9 and 10: carcinoid disease with right heart involvement.

1128 19a (TTE) and 19c (CMR): Restriction of the movements of the tricuspid leaflets, which are  
1129 thickened. The right ventricle myocardium is also involved

1130 19b: massive tricuspid regurgitation (TTE)

1131 19c: CMR showing dilatation of right heart cavities and restricted tricuspid leaflet (arrow)

1132 RA: right atrium, RV: right ventricle, LV: left ventricle, LA: left atrium

1133

1134 Figure 20: ASE / EACVI algorithm comparing constrictive pericarditis and restrictive  
1135 cardiomyopathy.

1136

1137 Figure 21: Multimodality imaging in a patient with constrictive pericarditis

1138 21a: CMR: Cine 4 chambers view in end-diastolic phase showing a circumferential pericardial  
1139 thickening (black arrows), biatrial dilatation and septal convexity inversion (open arrow)

1140 21b: Cardiac CT: Axial thoracic CT scan showing a circumferential pericardial thickening (black  
1141 arrows).

1142

1143 Video 11: CMR in constrictive pericarditis, illustrating the respiratory septal shift (difference in the  
1144 maximal septal excursion into LV between inspiration and expiration)

1145

1146 Figure 22 and video 12: left ventricular hypertrabeculation (arrows) in a young patient with severe  
1147 RCM

1148

1149

1150

1151

1152

1153

1154

1155

1156 **References**

1157

1158**1.** Elliott P, Andersson B, Arbustini E, Bilinska Z, Cecchi F, Charron P, et al. Classification of the  
1159 cardiomyopathies: a position statement from the European Society Of Cardiology Working Group on  
1160 Myocardial and Pericardial Diseases. *Eur Heart J.* 2008 ; 29:270-6.

1161

1162**2.** Richardson P, McKenna W, Bristow M, Maisch B, Mautner B, O'Connell J, et al. Report of the 1995  
1163 World Health Organization/International Society and Federation of Cardiology Task Force on the  
1164 Definition and Classification of cardiomyopathies. *Circulation.* 1996;93:841-2.

1165

1166**3.** Maron BJ, Towbin JA, Thiene G, Antzelevitch C, Corrado D, Arnett D, et al. Contemporary definitions  
1167 and classification of the cardiomyopathies: an American Heart Association Scientific Statement from  
1168 the Council on Clinical Cardiology, Heart Failure and Transplantation Committee; Quality of Care  
1169 and Outcomes Research and Functional Genomics and Translational Biology Interdisciplinary  
1170 Working Groups; and Council on Epidemiology and Prevention. *Circulation.* 2006;113:1807-16.

1171

1172**4.** Nihoyannopoulos P, Dawson D. Restrictive cardiomyopathies. *Eur J Echocardiogr* 2009 ; 10 : 23-33  
1173

1174**5.** Kushwaha SS, Fallon JT, Fuster V. Restrictive cardiomyopathy. *N Engl J Med.* 1997 ; 336:267-76.  
1175

1176**6.** Tam JW, Shaikh N, Sutherland E. Echocardiographic assessment of patients with hypertrophic and  
1177 restrictive cardiomyopathy: imaging and echocardiography. *Curr Opin Cardiol.* 2002;17:470-7.  
1178

1179**7.** Hancock EW. Differential diagnosis of restrictive cardiomyopathy and constrictive pericarditis. *Heart*  
1180 2001;86:343-9.

1181

1182**8.** Nagueh SF, Smiseth OA, Appleton CP, Byrd BF 3rd, Dokainish H, Edvardsen T, et al.  
1183 Recommendations for the Evaluation of Left Ventricular Diastolic Function by Echocardiography: An  
1184 Update from the American Society of Echocardiography and the European Association of  
1185 Cardiovascular Imaging. *Eur Heart J Cardiovasc Imaging* doi:10.1093/ehjci/jew082  
1186

1187**9.** Klein AL, Hatle LK, Taliercio CP, Oh JK, Kyle RA, Gertz MA, Bailey KR, Seward JB, Tajik AJ.  
1188 Prognostic significance of Doppler measures of diastolic function in cardiac amyloidosis. A Doppler  
1189 echocardiography study. *Circulation* 1991;83:808-816

1190

1191

- 1192**10.** Hyodo E, Hozumi T, Takemoto Y, et al. Early detection of cardiac involvement in patients with  
1193 sarcoidosis by a non-invasive method with ultrasonic tissue characterisation. *Heart* 2004;90:1275-  
1194 80.  
1195
- 1196**11.** Bhandari AK, Nanda NC. Myocardial texture characterization by two-dimensional  
1197 echocardiography. *Am J Cardiol* 1983; 51:817  
1198
- 1199**12.** Schiano-Lomoriello V, Galderisi M, Mele D, Esposito R, Cerciello G, Buonauro A, et al.  
1200 Longitudinal strain of left ventricular basal segments and E/e' ratio differentiate primary cardiac  
1201 amyloidosis at presentation from hypertensive hypertrophy: an automated function imaging study.  
1202 *Echocardiography*. 2016 Jun 9. doi: 10.1111/echo.13278  
1203
- 1204**13.** Sengupta PP, Krishnamoorthy VK, Abhayaratna WP, Korinek J, Belohlavek M, Sundt TM 3rd,  
1205 et al. Disparate patterns of left ventricular mechanics differentiate constrictive pericarditis from  
1206 restrictive cardiomyopathy. *JACC Cardiovasc Imaging* 2008;**1**:29-38.
- 1207**14.** Kramer CM, Barkhausen J, Flamm SD, Kim RJ, Nagel E; Society for Cardiovascular Magnetic  
1208 Resonance Board of Trustees Task Force on Standardized Protocols. Standardized cardiovascular  
1209 magnetic resonance (CMR) protocols 2013 update. *J Cardiovasc Magn Reson*. 2013 Oct 8;15:91  
1210
- 1211**15.** Bellenger NG, Davies LC, Francis JM, Coats AJ, Pennell DJ. Reduction in sample size for  
1212 studies of remodeling in heart failure by the use of cardiovascular magnetic resonance. *J Cardiovasc*  
1213 *Magn Reson*. 2000;2(4):271-8.  
1214
- 1215**16.** Cosyns B, Plein S, Nihoyanopoulos P, Smiseth O, Achenbach S, Andrade MJ, et al. European  
1216 Association of Cardiovascular Imaging (EACVI); European Society of Cardiology Working Group (ESC  
1217 WG) on Myocardial and Pericardial diseases. European Association of Cardiovascular Imaging  
1218 (EACVI) position paper: Multimodality imaging in pericardial disease. *Eur Heart J Cardiovasc*  
1219 *Imaging*. 2015;16:12-31.  
1220
- 1221**17.** Franccone M, Dymarkowski S, Kalantzi M, Rademakers FE, Bogaert J. Assessment of  
1222 ventricular coupling with real-time cine MRI and its value to differentiate constrictive pericarditis  
1223 from restrictive cardiomyopathy. *Eur Radiol*. 2006;16:944-51  
1224
- 1225**18.** Sado DM, White SK, Piechnik SK, Banyersad SM, Treibel T, Captur G, et al. Identification  
1226 and assessment of Anderson-Fabry disease by cardiovascular magnetic resonance noncontrast  
1227 myocardial T1 mapping. *Circ Cardiovasc Imaging*. 2013;6:392-8  
1228

1229**19.** Fontana M, Pica S, Reant P, Abdel-Gadir A, Treibel TA, Banypersad SM, et al. Prognostic Value  
1230 of Late Gadolinium Enhancement Cardiovascular Magnetic Resonance in Cardiac Amyloidosis.  
1231 *Circulation*. 2015;132:1570-9  
1232

1233**20.** Schelbert EB, Piehler KM, Zareba KM, Moon JC, Ugander M, Messroghli DR, et al. Myocardial  
1234 Fibrosis Quantified by Extracellular Volume Is Associated With Subsequent Hospitalization for Heart  
1235 Failure, Death, or Both Across the Spectrum of Ejection Fraction and Heart Failure Stage. *J Am*  
1236 *Heart Assoc*. 2015;4: 12.  
1237

1238**21.** Anderson LJ, Holden S, Davis B, Prescott E, Charrier CC, Bunce NH, et al. Cardiovascular  
1239 T2-star (T2\*) magnetic resonance for the early diagnosis of myocardial iron overload. *Eur Heart J*.  
1240 2001 ;22:2171-9.  
1241

1242**22.** Modell B, Khan M, Darlison M, Westwood MA, Ingram D, Pennell DJ. Improved survival of  
1243 thalassaemia major in the UK and relation to T2\* cardiovascular magnetic resonance. *J Cardiovasc*  
1244 *Magn Reson*. 2008;10:42  
1245

1246**23.** Karamitsos TD, Piechnik SK, Banypersad SM, Fontana M, Ntusi NB, Ferreira VM, et al.  
1247 Noncontrast T1 mapping for the diagnosis of cardiac amyloidosis. *JACC Cardiovasc Imaging*. 2013  
1248 ;6:488-97  
1249

1250**24.** Banypersad SM, Sado DM, Flett AS, Gibbs SD, Pinney JH, Maestrini V, et al. Quantification  
1251 of myocardial extracellular volume fraction in systemic AL amyloidosis: an equilibrium contrast  
1252 cardiovascular magnetic resonance study. *Circ Cardiovasc Imaging*. 2013;6:34-9.  
1253

1254**25.** Alam MH, Auger D, McGill LA, Smith GC, He T, Izgi C, et al. Comparison of 3 T and 1.5 T for  
1255 T2\* magnetic resonance of tissue iron. *J Cardiovasc Magn Reson*. 2016;18:40  
1256

1257**26.** Yared K, Baggish AL, Picard MH, Hoffmann U, Hung J. Multimodality imaging of pericardial  
1258 diseases. *JACC Cardiovascular imaging*. 2010;3:650-660.  
1259

1260**27.** Zhao L, Ma X, Feuchtner GM, Zhang C, Fan Z. Quantification of myocardial delayed  
1261 enhancement and wall thickness in hypertrophic cardiomyopathy: multidetector computed  
1262 tomography versus magnetic resonance imaging. *European journal of radiology*. 2014;**83**:1778-1785.  
1263

1264**28.** Hamilton-Craig C, Seltmann M, Ropers D, Achenbach S. Myocardial viability by dual-energy  
1265 delayed enhancement computed tomography. *JACC Cardiovascular imaging*. 2011;**4**:207-208.  
1266

- 1267**29.** Bandula S, Banypersad SM, Sado D, Flett AS, Punwani S, Taylor SA, et al. Measurement of  
1268 Tissue Interstitial Volume in Healthy Patients and Those with Amyloidosis with Equilibrium Contrast-  
1269 enhanced MR Imaging. *Radiology*. Radiological Society of North America, Inc; 2013;**268**:858–864.  
1270
- 1271**30.** Kula RW, Engel WK, Line BR. Scanning for soft-tissue amyloid. *Lancet* 1977 ; 1:92–3  
1272
- 1273**31.** Aljaroudi WA, Desai MY, Tang WH, Phelan D, Cerqueira MD, Jaber WA. Role of imaging in the  
1274 diagnosis and management of patients with cardiac amyloidosis: state of the art review and focus on  
1275 emerging nuclear techniques. *J Nucl Cardiol*. 2014;21:271-83  
1276
- 1277**32.** Glaudemans AW, van Rheenen RW, van den Berg MP, et al. Bone scintigraphy with  
1278 (99m)technetium-hydroxymethylene diphosphonate allows early diagnosis of cardiac involvement in  
1279 patients with transthyretin-derived systemic amyloidosis. *Amyloid* 2014; **21**: 35-44.  
1280
- 1281**33.** Minutoli F, Di Bella G, Mazzeo A, Donato R, Russo M, Scribano E, et al. Comparison between  
1282 (99m)Tc-diphosphonate imaging and MRI with late gadolinium enhancement in evaluating cardiac  
1283 involvement in patients with transthyretin familial amyloid polyneuropathy. *AJR Am J Roentgenol*  
1284 2013;200:W256-65.  
1285
- 1286**34.** Coutinho MC, Cortez-Dias N, Cantinho G, Conceição I, Oliveira A, Bordalo e Sá A, et al.  
1287 Reduced myocardial 123-iodine metaiodobenzylguanidine uptake: a prognostic marker in familial  
1288 amyloid polyneuropathy. *Circ Cardiovasc Imaging*. 2013;6:627-36.  
1289
- 1290**35.** Youssef G, Beanlands RSB, Birnie DH, Nery PB. Cardiac sarcoidosis: applications of imaging  
1291 in diagnosis and directing treatment. *Heart*. 2011;97(24):2078–87.  
1292
- 1293**36.** Ohira H, Tsujino I, Ishimaru S, et al. Myocardial imaging with 18F-fluoro-2-deoxyglucose  
1294 positron emission tomography and magnetic resonance imaging in sarcoidosis. *Eur J Nucl Med Mol*  
1295 *Imaging*. 2008;35(5):933–41.  
1296  
1297
- 1298**37.** **Apgral RD**weck MR, Trivieri MG, Robson PM, Karakatsanis N, Mani V, et al. Clinical Utility  
1299 of Combined FDG-PET/MR to Assess Myocardial Disease. *JACC Imaging*. 2016. Epub pii: S1936-  
1300 878X(16)30259-5  
1301
- 1302**38.** Mogensen J, Arbustini E. Restrictive cardiomyopathy. *Curr Opin Cardiol* 2009;24:214-20.  
1303

1304**39.** Arbustini E, Morbini P, Grasso M, et al. Restrictive cardiomyopathy, atrioventricular block  
1305 and mild to subclinical myopathy in patients with desmin-immunoreactive material deposits. *J Am*  
1306 *Coll Cardiol* 1998;31:645-53.  
1307

1308**40.** Arbustini E, Buonanno C, Trevi G, Pennelli N, Ferrans VJ, Thiene G. Cardiac ultrastructure  
1309 in primary restrictive cardiomyopathy. *Chest* 1983;84:236-8.  
1310

1311**41.** Cannavale A, Ordovas KG, Rame EJ, Higgins CB. Hypertrophic cardiomyopathy with  
1312 restrictive phenotype and myocardial crypts. *J Thorac Imaging* 2010;25:W121-3.  
1313

1314**42.** Rapezzi C, Lorenzini M, Longhi S, et al. Cardiac amyloidosis: the great pretender. *Heart Fail*  
1315 *Rev* 2015; **20**: 117-24  
1316

1317**43.** Rapezzi C, Arbustini E, Caforio AL, et al. Diagnostic work-up in cardiomyopathies: bridging  
1318 the gap between clinical phenotypes and final diagnosis. A position statement from the ESC Working  
1319 Group on Myocardial and Pericardial Diseases. *Eur Heart J.* 2013;34:1448-58.  
1320

1321**44.** Koyama J, Ikeda S, Ikeda U. Echocardiographic assessment of the cardiac amyloidoses. *Circ*  
1322 *J* 2015; **79**: 721-34.  
1323

1324**45.** Feng D, Edwards WD, Oh JK, et al. Intracardiac thrombosis and embolism in patients with  
1325 cardiac amyloidosis. *Circulation* 2007; **116**: 2420-6.  
1326

1327**46.** Innelli P, Galderisi M, Catalano L, Martorelli MC, Olibet M, Pardo M, et al.. Detection of  
1328 increased left ventricular filling pressure by pulsed tissue Doppler in cardiac amyloidosis. *J*  
1329 *Cardiovasc Med* 2006 ;7 :742-7  
1330

1331**47.** Tendler A, Helmke S, Teruya S, Alvarez J, Maurer MS. The myocardial contraction fraction is  
1332 superior to ejection fraction in predicting survival in patients with AL cardiac amyloidosis. *Amyloid*  
1333 2015; **22**: 61-6.  
1334

1335**48.** Phelan D, Collier P, Thavendiranathan P, et al. Relative apical sparing of longitudinal strain  
1336 using two-dimensional speckle-tracking echocardiography is both sensitive and specific for the  
1337 diagnosis of cardiac amyloidosis. *Heart* 2012; **98**: 1442-8.  
1338

1339**49.** Schiano-Lomoriello V, Galderisi M, Mele D, Esposito R, Cerciello G, Buonauro A, et al.  
1340 Longitudinal strain of left ventricular basal segments and E/e' ratio differentiate primary cardiac  
1341 amyloidosis at presentation from hypertensive hypertrophy: an automated function imaging study.  
1342 *Echocardiography.* 2016;33:1335-43



1343

1344**50.** Bellavia D, Pellikka PA, Al-Zahrani GB, et al. Independent predictors of survival in primary systemic  
1345 (Al) amyloidosis, including cardiac biomarkers and left ventricular strain imaging: an observational  
1346 cohort study. *J Am Soc Echocardiogr* 2010; **23**: 643-52.

1347

1348**51.** Ternacle J, Bodez D, Guellich A, et al. Causes and Consequences of Longitudinal LV Dysfunction  
1349 Assessed by 2D Strain Echocardiography in Cardiac Amyloidosis. *JACC Cardiovasc Imaging*.  
1350 2016;9:126-38

1351

1352**52.** Quarta CC, Solomon SD, Uraizee I, Kruger J, Longhi S, Ferlito M, et al. Left Ventricular Structure  
1353 and Function in TTR-Related versus AL Cardiac Amyloidosis. *Circulation*. 2014;129:1840-9

1354

1355**53.** Maceira AM, Joshi J, Prasad SK, et al. Cardiovascular magnetic resonance in cardiac amyloidosis.  
1356 *Circulation* 2005; **111**: 186-93.

1357

1358**54.** Vogelsberg H, Mahrholdt H, Deluigi CC, et al. Cardiovascular magnetic resonance in clinically  
1359 suspected cardiac amyloidosis: noninvasive imaging compared to endomyocardial biopsy. *J Am Coll*  
1360 *Cardiol* 2008; **51**: 1022-30.

1361

1362**55.** Syed IS, Glockner JF, Feng D, et al. Role of cardiac magnetic resonance imaging in the detection of  
1363 cardiac amyloidosis. *JACC Cardiovasc Imaging* 2010; **3**: 155-64.

1364

1365**56.** Fontana M, Pica S, Reant P, et al. Prognostic Value of Late Gadolinium Enhancement Cardiovascular  
1366 Magnetic Resonance in Cardiac Amyloidosis. *Circulation* 2015; **132**: 1570-9.

1367

1368**57.** Karamitsos TD, Piechnik SK, Banyersad SM, et al. Noncontrast T1 mapping for the diagnosis of  
1369 cardiac amyloidosis. *JACC Cardiovasc Imaging* 2013; **6**: 488-97.

1370

1371**58.** Fontana M, Banyersad SM, Treibel TA, et al. Differential Myocyte Responses in Patients with Cardiac  
1372 Transthyretin Amyloidosis and Light-Chain Amyloidosis: A Cardiac MR Imaging Study. *Radiology*  
1373 2015; **277**: 388-97.

1374

1375**59.** Di Bella G, Pizzino F, Minutoli F, et al. The mosaic of the cardiac amyloidosis diagnosis: role of  
1376 imaging in subtypes and stages of the disease. *Eur Heart J Cardiovasc Imaging* 2014; **15**: 1307-15.

1377

1378**60.** Bokhari S, Castano A, Pozniakoff T, Deslisle S, Latif F, Maurer MS. (99m)Tc-pyrophosphate  
1379 scintigraphy for differentiating light-chain cardiac amyloidosis from the transthyretin-related familial  
1380 and senile cardiac amyloidoses. *Circ Cardiovasc Imaging* 2013; **6**: 195-201.

- 1381
- 1382 **61.** Hutt DF, Quigley AM, Page J, et al. Utility and limitations of 3,3-diphosphono-1,2-  
1383 propanodicarboxylic acid scintigraphy in systemic amyloidosis. *Eur Heart J Cardiovasc Imaging* 2014;  
1384 **15**: 1289-98.
- 1385
- 1386 **62.** Perugini E, Guidalotti PL, Salvi F, et al. Noninvasive etiologic diagnosis of cardiac amyloidosis using  
1387 <sup>99m</sup>Tc-3,3-diphosphono-1,2-propanodicarboxylic acid scintigraphy. *J Am Coll Cardiol*.  
1388 2005;46:1076-84.
- 1389
- 1390 **63.** Rapezzi C, Quarta CC, Guidalotti PL, Pettinato C, Fanti S, Leone O, et al. Role of (<sup>99m</sup>)Tc-DPD  
1391 scintigraphy in diagnosis and prognosis of hereditary transthyretin-related cardiac amyloidosis.  
1392 *JACC Cardiovasc Imaging* 2011;4:659-70.
- 1393
- 1394 **64.** Gillmore JD, Maurer MS, Falk RH, et al. Nonbiopsy diagnosis of cardiac transthyretin amyloidosis.  
1395 *Circulation* 2016 ; 133 : 2404-12.
- 1396
- 1397 **65.** Cardim N, Galderisi M, Edvardsen T, et al. Role of multimodality cardiac imaging in the management  
1398 of patients with hypertrophic cardiomyopathy: an expert consensus of the European Association of  
1399 Cardiovascular Imaging Endorsed by the Saudi Heart Association. *Eur Heart J Cardiovasc Imaging*  
1400 2015; **16**: 280.
- 1401
- 1402
- 1403 **66.** Bosi G, Crepaz R, Gamberini MR, Fortini M, Scarcia S, Bonsante E, Pitscheider W, Vaccari M. Left  
1404 ventricular remodelling, and systolic and diastolic function in young adults with beta thalassaemia  
1405 major: a Doppler echocardiographic assessment and correlation with haematological data. *Heart*.  
1406 2003;89:762-766.
- 1407
- 1408 **67.** Leon MB, Borer JS, Bacharach SL, Green MV, Benz EJ Jr, Griffith P, Nienhuis AW.  
1409 Detection of early cardiac dysfunction in patients with severe beta-thalassemia and chronic  
1410 iron overload. *N Engl J Med*. 1979;301:1143-1148.
- 1411
- 1412 **68.** Kremastinos DT, Farmakis D, Aessopos A, Hahalis G, Hamodraka E, Tsiapras D, Keren  
1413 A. Beta-thalassemia cardiomyopathy: history, present considerations, and future  
1414 perspectives. *Circ Heart Fail*. 2010;3:451-458.
- 1415
- 1416 **69.** Cogliandro T, Derchi G, Mancuso L, Mayer MC, Pannone B, Pepe A, Pili M, Bina P,  
1417 Cianciulli P, De Sanctis V, Maggio A; Society for the Study of Thalassemia and  
1418 Hemoglobinopathies (SoSTE). Guideline recommendations for heart complications in  
1419 thalassemia major. *J Cardiovasc Med*. 2008;9:515-525.

- 1420 **70.** Eftimiadis GK, Hassapopoulou HP, Tsikaderis DD, Karvounis HI, Giannakoulas GA,  
1421 Parharidis GE, Louridas GE. Survival in thalassaemia major patients. *Circ J.* 2006;70:1037-  
1422 1042.  
1423
- 1424 **71.** Giakoumis A, Berdoukas V, Gotsis E, Aessopos A. Comparison of echocardiographic  
1425 (US) volumetry with cardiac magnetic resonance imaging in transfusion dependent  
1426 thalassemia major. *Cardiovasc Ultrasound.* 2007;5:24  
1427
- 1428 **72.** Pennell DJ, Udelson JE, Arai AE, Bozkurt B, Cohen AR, Galanello R, et al; American  
1429 Heart Association Committee on Heart Failure and Transplantation of the Council on Clinical  
1430 Cardiology and Council on Cardiovascular Radiology and Imaging. Cardiovascular function  
1431 and treatment in  $\beta$ -thalassemia major: a consensus statement from the American Heart  
1432 Association. *Circulation.* 2013;128:281-308.  
1433
- 1434 **73.** Pepe A, Meloni A, Capra M, Cianciulli P, Prossomariti L, Malaventura C, et al.  
1435 Deferasirox, deferiprone and desferrioxamine treatment in thalassemia major patients:  
1436 cardiac iron and function comparison determined by quantitative magnetic resonance  
1437 imaging. *Haematologica* 2011;96:41-47.  
1438
- 1439 **74.** Meloni A, Positano V, Ruffo GB, Spasiano A, D'Ascola D, Peluso A, et al. Improvement  
1440 of heart iron with preserved patterns of iron store by CMR-guided chelation therapy *European*  
1441 *Heart Journal - Cardiovascular Imaging* 2015:325-34.  
1442
- 1443 **75.** Casale M, Meloni A, Filosa A, Cuccia L, Caruso V, Palazzi G, et al. Multiparametric  
1444 Cardiac Magnetic Resonance Survey in Children With Thalassemia Major A Multicenter  
1445 Study. *Circ Cardiovasc Imaging.* 2015; 8:e003230. doi: 10.1161/CIRCIMAGING.115.003230.  
1446
- 1447 **76.** Pepe A, Positano V, Capra M, Maggio A, Pinto CL, Spasiano A, et al. Myocardial  
1448 scarring by delayed enhancement cardiovascular magnetic resonance in thalassaemia major.  
1449 *Heart.* 2009;95:1688-1693.  
1450
- 1451 **77.** Linhart A, Kampmann C, Zamorano JL, Sunder-Plassmann G, Beck M, Mehta A, et al.  
1452 European FOS Investigators Cardiac manifestations of Anderson-Fabry disease: results from  
1453 the international Fabry outcome survey.. *Eur Heart J.* 2007; 28:1228-35  
1454
- 1455 **78.** MacDermot KD, Holmes A, Miners AH. Natural history of Fabry disease in affected  
1456 males and obligate carrier females. *J Inher Metab Dis.* 2001;24 Suppl 2:13-4  
1457

- 1458 **79.** Gambarin FI, Disabella E, Narula J, Diegoli M, Grasso M, Serio A, et al. When should  
1459 cardiologists suspect Anderson-Fabry disease? *Am J Cardiol.* 2010 ;106:1492-9  
1460
- 1461 **80.** West M, Nicholls K, Mehta A, Clarke JT, Steiner R, Beck M, et al. Agalsidase alpha and  
1462 kidney dysfunction in Fabry disease. *J Am Soc Nephrol.* 2009;20:1132-9.  
1463
- 1464 **81.** Perrot A, Osterziel KJ, Beck M, Dietz R, Kampmann C. Fabry disease: focus on cardiac  
1465 manifestations and molecular mechanisms. *Herz.* 2002;27(7):699-702  
1466
- 1467 **82.** Nagueh SF. Anderson-Fabry disease and other lysosomal storage disorders.  
1468 *Circulation* 2014; 130: 1081-90  
1469
- 1470 **83.** Weidemann F, Linhart A, Monserrat L, Strotmann J. Cardiac challenges in patients  
1471 with Fabry disease. *Int J Cardiol.* 2010 ;14:141:3-10  
1472
- 1473 **84.** Hoigné P, Attenhofer Jost CH, Duru F, Oechslin EN, Seifert B, Widmer U, et al. Simple  
1474 criteria for differentiation of Fabry disease from amyloid heart disease and other causes of left  
1475 ventricular hypertrophy. *Int J Cardiol.* 2006 ;111:413-22  
1476
- 1477 **85.** Feriozzi S, Schwarting A, Sunder-Plassmann G, West M, Cybulla M; International  
1478 Fabry Outcome Survey Investigators. Agalsidase alpha slows the decline in renal function in  
1479 patients with Fabry disease. *Am J Nephrol.* 2009;29:353-61  
1480
- 1481 **86.** Pieroni M, Chimenti C, Russo A, Russo MA, Maseri A, Frustaci A. Tissue Doppler  
1482 imaging in Fabry disease. *Curr Opin Cardiol.* 2004;19:452-7  
1483
- 1484 **87.** Toro R, Perez-Isla L, Doxastaquis G, Barba MA, Gallego AR, Pintos G, et al. Clinical  
1485 usefulness of tissue Doppler imaging in predicting preclinical Fabry cardiomyopathy. *Int J*  
1486 *Cardiol.* 2009;132:38-44  
1487
- 1488 **88.** Zamorano J, Serra V, Pérez de Isla L, Feltes G, Calli A, Barbado FJ, et al. Usefulness  
1489 of tissue Doppler on early detection of cardiac disease in Fabry patients and potential role of  
1490 enzyme replacement therapy (ERT) for avoiding progression of disease.. *Eur J Echocardiogr.*  
1491 2011;12:671-7  
1492
- 1493 **89.** De Cobelli F, Esposito A, Belloni E, Pieroni M, Perseghin G, Chimenti C, et al. Delayed-  
1494 enhanced cardiac MRI for differentiation of Fabry's disease from symmetric hypertrophic  
1495 cardiomyopathy. *AJR Am J Roentgenol.* 2009 ;192:W97-102

1496  
1497 **90.** Sado DM, White SK, Piechnik SK, Banypersad SM, Treibel T, Captur G, et al.  
1498 Identification and assessment of Anderson-Fabry disease by cardiovascular magnetic  
1499 resonance noncontrast myocardial T1 mapping. *Circ Cardiovasc Imaging*. 2013;6:392-8.  
1500  
1501 **91.** Boucek D, Jirikowic J, Taylor M. Natural history of Danon disease. *Genet Med*.  
1502 2011;13:563-568  
1503  
1504 **92.** Maron BJ, Roberts WC, Arad M, Haas TS, Spirito P, Wright GB, et al. Clinical outcome  
1505 and phenotypic expression in LAMP2 cardiomyopathy. *JAMA*. 2009;301:1253-1259  
1506  
1507 **93.** D'souza RS, Levandowski C, Slavov D, Graw SL, Allen LA, Adler E, et al. Danon  
1508 disease: clinical features, evaluation, and management. *Circ Heart Fail*. 2014;7:843-9  
1509  
1510 **94.** Gussenhoven WJ, Busch HF, Kleijer WJ, de Villeneuve VH. Echocardiographic  
1511 features in the cardiac type of glycogen storage disease II. *Eur Heart J*. 1983;4:41-3  
1512  
1513 **95.** Rees A, Elbl F, Minhas K, Solinger R. Echocardiographic evidence of outflow tract  
1514 obstruction in Pompe's disease (glycogen storage disease of the heart). *Am J Cardiol*. 1976  
1515 ;37:1103-6.  
1516  
1517 **96.** Barker PC, Pasquali SK, Darty S, Ing RJ, Li JS, Kim RJ, et al. Use of cardiac magnetic  
1518 resonance imaging to evaluate cardiac structure, function and fibrosis in children with  
1519 infantile Pompe disease on enzyme replacement therapy. *Mol Genet Metab*. 2010;101:332-7  
1520  
1521 **97.** Nucifora G, Miani D, Piccoli G, Proclemer A. Cardiac magnetic resonance imaging in  
1522 Danon disease. *Cardiology*. 2012;121:27-30  
1523  
1524 **98.** Wei LG, Gao JQ, Liu XM, Huang JM, Li XZ. A study of glycogen storage disease with  
1525 <sup>99</sup>Tcm-MIBI gated myocardial perfusion imaging. *Ir J Med Sci*. 2013 Dec;182:615-20  
1526  
1527 **99.** Lo Iudice F, Barbato A, Muscariello R, Di Nardo C, de Stefano F, Sibilio M, et al . Left  
1528 Ventricular Diastolic Dysfunction in Type I Gaucher Disease: An Echo Doppler Study.  
1529 *Echocardiography* 2015;32:890-895  
1530  
1531 **100.** Braunlin E, Wang R. Cardiac issues in adults with mucopolysaccharidoses; current  
1532 knowledge and emerging needs. *Heart* 2016; 102:1257-1262  
1533

- 1534 **101.** Przybojewski JZ, Maritz F, Tiedt FA, van der Walt JJ. Pseudoxanthoma elasticum with  
1535 cardiac involvement. A case report and review of the literature. *S Afr Med J.* 1981;59:268-75.  
1536
- 1537 **102.** Campens L, Vanakker OM, Trachet B, Segers P, Leroy BP, De Zaeytijd J et al.  
1538 Characterization of cardiovascular involvement in pseudoxanthoma elasticum families.  
1539 *Arterioscler Thromb Vasc Biol.* 2013;33:2646-52  
1540
- 1541 **103.** Nguyen LD, Terbah M, Daudon P, Martin L. Left ventricular systolic and diastolic  
1542 function by echocardiogram in pseudoxanthoma elasticum. *Am J Cardiol.* 2006;97:1535-7  
1543
- 1544 **104.** Sabán-Ruiz J, Fabregate Fuente R, Sánchez-Largo Uceda E, Fabregate Fuente M.  
1545 Pseudoxanthoma elasticum: case report with arterial stiffness evaluated by a research  
1546 cardiovascular profiling system. *Eur J Dermatol.* 2010;20:785-7  
1547
- 1548 **105.** Kandolin R, Lehtonen J, Airaksinen J, Vihinen T, Miettinen H, Ylitalo K, et al. Cardiac  
1549 sarcoidosis: epidemiology, characteristics, and outcome over 25 years in a nationwide study.  
1550 *Circulation.* 2015;131:624-32  
1551
- 1552 **106.** Birnie DH, Sauer WH, Bogun F, Cooper JM, Culver DA, Duvernoy CS et al. HRS expert  
1553 consensus statement on the diagnosis and management of arrhythmias associated with  
1554 cardiac sarcoidosis. *Heart Rhythm* 2014; 11:1305-1323  
1555
- 1556 **107.** Judson MA, Costabel U, Drent M, Wells A, Maier L, Koth L et al. Organ Assessment  
1557 Instrument Investigators TW. The WASOG Sarcoidosis Organ Assessment Instrument: An  
1558 update of a previous clinical tool. *Sarcoidosis Vasc Diffuse Lung Dis.* 2014;31:19-27.  
1559
- 1560 **108.** Chiu CZ, , Nakatani S, Yamagishi M, Miyatake K, Cheng JJ. Echocardiographic  
1561 Manifestations in Patients with Cardiac Sarcoidosis, *J Med Ultrasound* 2002; 10:135-140.  
1562
- 1563 **109.** Hourigan L.A., Burstow D.J., Pohlner P., Clarke B.E., Donnelly J.E. Transesophageal  
1564 echocardiographic abnormalities in a case of cardiac sarcoidosis. *J Am Soc Echocardiogr.*  
1565 2001;14:399-402  
1566
- 1567 **110.** Patel MR, Cawley PJ, Heitner JF, Klem I, Parker MA, Jaroudi WA. Detection of  
1568 myocardial damage in patients with sarcoidosis. *Circulation.* 2009 ;120:1969-77.  
1569
- 1570 **111.** Hundley WG, Bluemke DA, Finn JP, Flamm SD, Fogel MA, Friedrich MG et al.  
1571 ACCF/ACR/AHA/NASCI/SCMR 2010 expert consensus document on cardiovascular

1572 magnetic resonance: a report of the American College of Cardiology Foundation Task Force  
1573 on Expert Consensus Documents. *J Am Coll Cardiol.* 2010;55:2614-62.  
1574

1575 **112.** J Schulz-Menger, R Wassmuth, H Abdel-Aty, I Siegel, A Franke, R Dietz, M G Friedrich.  
1576 Patterns of myocardial inflammation and scarring in sarcoidosis as assessed by  
1577 cardiovascular magnetic resonance *Heart* 2006;92:399-400.  
1578

1579 **113.** Seward JB, Casacang-Verzosa G. Infiltrative cardiovascular diseases:  
1580 cardiomyopathies that look alike. *J Am Coll Cardiol.* 2010;55:1769-79.  
1581

1582 **114.** Lancefield T, Voskoboinik A, Taylor AJ, Nadel J Late gadolinium enhancement  
1583 identified with cardiac magnetic resonance imaging in sarcoidosis patients is associated with  
1584 long-term ventricular arrhythmia and sudden cardiac death., *Eur Heart J Cardiovasc*  
1585 *Imaging.* 2015 ;16:634-41.  
1586

1587 **115.** Okumura W, Iwasaki T, Toyama T, Iso T, Arai M, Oriuchi N, Endo K, Yokoyama T,  
1588 Suzuki T, Kurabayashi M. Usefulness of fasting 18F-FDG PET in identification of cardiac  
1589 sarcoidosis. *J Nucl Med.* 2004 ;45:1989-98  
1590

1591 **116.** Keijsers RG, Grutters JC, Thomeer M, Du Bois RM, Van Buul MM, Lavalaye et al.  
1592 Imaging the inflammatory activity of sarcoidosis: sensitivity and inter observer agreement of  
1593 (67)Ga imaging and (18)F-FDG PET. *Q J Nucl Med Mol Imaging.* 2011;55:66-71  
1594

1595 **117.** Ishimaru S, Tsujino I, Takei T, Tsukamoto E, Sakaue S, Kamigaki M, et al. Focal  
1596 uptake on 18F-fluoro-2-deoxyglucose positron emission tomography images indicates cardiac  
1597 involvement of sarcoidosis. *Eur Heart J.* 2005;26:1538-43.  
1598

1599 **118.** Youssef G, Leung E, Mylonas I, Nery P, Williams K, Wisenberg G, et al. The use of 18F-  
1600 FDG PET in the diagnosis of cardiac sarcoidosis: a systematic review and metaanalysis  
1601 including the Ontario experience. *J Nucl Med.* 2012;53:241-8  
1602

1603 **119.** Tang R, Wang JT, Wang L, Le K, Huang Y, Hickey AJ, Emmett L. Impact of Patient  
1604 Preparation on the Diagnostic Performance of 18F-FDG PET in Cardiac Sarcoidosis: A  
1605 Systematic Review and Meta-analysis. *Clin Nucl Med.* 2015 Dec 4.  
1606

1607 **120.** Skali H, Schulman AR, Dorbala S. (18)F-FDG PET/CT for the assessment of  
1608 myocardial sarcoidosis. *Curr Cardiol Rep* 2013; 15:352.  
1609

- 1610 **121.** Blankstein R, Osborne M, Naya M, Waller A, Kim CK, Murthy VL et al. Cardiac positron  
1611 emission tomography enhances prognostic assessments of patients with suspected cardiac  
1612 sarcoid. *J Am Coll Cardiol.* 2014;63:329-36  
1613
- 1614 **122.** Yokoyama R, Miyagawa M, Okayama H, Inoue T, Miki H, Ogimoto A, Higaki J,  
1615 Mochizuki T. Quantitative analysis of myocardial 18F-fluorodeoxyglucose uptake by PET/CT  
1616 for detection of cardiac sarcoidosis. *Int J Cardiol.* 2015;195:180-7  
1617
- 1618 **123.** Yamagishi H, Shirai N, Takagi M, Yoshiyama M, Akioka K, Takeuchi K, Yoshikawa J.  
1619 Identification of cardiac sarcoidosis with (13) N-NH(3)/[18F]FDG PET. *J Nucl Med.*  
1620 2003;44:1030-6  
1621
- 1622 **124.** Osborne MT1, Hulten EA, Singh A, Waller AH, Bittencourt MS, Stewart GC, et al.  
1623 Reduction in <sup>18</sup>F-fluorodeoxyglucose uptake on serial cardiac positron emission tomography  
1624 is associated with improved left ventricular ejection fraction in patients with cardiac  
1625 sarcoidosis. *J Nucl Cardiol.* 2014 ;21:166-74.  
1626
- 1627 **125.** Ohira H, Birnie DH, Pena E, Bernick J, Mc Ardle B, Leung E, et al. Comparison of  
1628 (18)F-fluorodeoxyglucose positron emission tomography (FDG PET) and cardiac magnetic  
1629 resonance (CMR) in corticosteroid-naive patients with conduction system disease due to  
1630 cardiac sarcoidosis. *Eur J Nucl Med Mol Imaging.* 2016;43:259-69.  
1631
- 1632 **126.** Leask A. The role of endothelin-1 signaling in the fibrosis observed in systemic  
1633 sclerosis. *Pharmacol Res* 2011;63:502-503.  
1634
- 1635 **127.** Tyndall AJ, Bannert B, Vonk M, Airo P, Cozzi F, Carreira PE, et, al. Causes and risk  
1636 factors for death in systemic sclerosis: a study from the EULAR Scleroderma Trials and  
1637 Research (EUSTAR) database. *Ann Rheum Dis* 2010;69:1809-15.  
1638
- 1639 **128.** Follansbee WP, Miller TR, Cirtoss EI, Orié JE, Bernstein RL, Kiernan JM, et al. A  
1640 controlled clinicopathologic study of myocardial fibrosis in systemic sclerosis (scleroderma).  
1641 *J Rheumatol* 1990;17:656-62.  
1642
- 1643 **129.** Meune C, Avouac J, Wahbi K, et al. Cardiac involvement in systemic sclerosis assessed  
1644 by tissue-doppler echocardiography during routine care: A controlled study of 100  
1645 consecutive patients. *Arthritis Rheum* 2008;58(6):1803-1809.  
1646
- 1647 **130.** Allanore Y, Meune C, Vonk MC, Airo P, Hachulla E, Caramaschi P, et al. Prevalence  
1648 and factors associated with left ventricular dysfunction in the EULAR Scleroderma Trial and



- 1649 Research group (EUSTAR) database of patients with systemic sclerosis. *Ann Rheum Dis*  
1650 2010;69:218–21.  
1651
- 1652 **131.** D’Andrea A, Stisi S, Bellissimo S, Vigorito F, Scotto di Uccio F, Tozzi N, et al. Early  
1653 impairment of myocardial function in systemic sclerosis: non-invasive assessment by Doppler  
1654 myocardial and strain rate imaging. *Eur J Echocardiogr* 2005;6:407–18.  
1655
- 1656 **132.** Yiu KH, Schouffoer AA, Marsan NA, Ninaber MK, Stolk J, Vlieland TV, et al. Left  
1657 ventricular dysfunction assessed by speckle-tracking strain analysis in patients with systemic  
1658 sclerosis. *Arthritis Rheum* 2011;63: 3969–3978.  
1659
- 1660 **133.** Mueller KA, Mueller II, Eppler D, Zuern CS, Seizer P, Kramer U, et al. Clinical and  
1661 histopathological features of patients with systemic sclerosis undergoing endomyocardial  
1662 biopsy. *PLoS One*. 2015 May 12;10(5):e0126707. doi: 10.1371/journal.pone.0126707.  
1663 eCollection 2015. PubMed PMID: 25966025; PubMed Central PMCID: PMC4428754.  
1664
- 1665 **134.** Hachulla AL, Launay D, Gaxotte V, et al. Cardiac magnetic resonance imaging in  
1666 systemic sclerosis: a cross-sectional observational study of 52 patients. *Ann Rheum Dis*  
1667 2009;68(12):1878–1884.  
1668
- 1669 **135.** Ugander M, Oki AJ, Hsu LY, et al. Extracellular volume imaging by magnetic resonance  
1670 imaging provides insights into overt and sub-clinical myocardial pathology. *Eur Heart J*  
1671 2012;33:1268–1278.  
1672
- 1673 **136.** Barison A, Gargani L, De Marchi D, Aquaro GD, Guiducci S, Picano E, et al. Early  
1674 myocardial and skeletal muscle interstitial remodelling in systemic sclerosis: insights from  
1675 extracellular volume quantification using cardiovascular magnetic resonance. *Eur Heart J*  
1676 *Cardiovasc Imaging*. 2015;16:74–80.  
1677
- 1678 **137.** Thuny F, Lovric D, Schnell F, Bergerot C, Ernande L, Cottin V, et al. Quantification of  
1679 myocardial extracellular volume fraction with cardiac MR imaging for early detection of left  
1680 ventricle involvement in systemic sclerosis. *Radiology*. 2014;271:373–80.  
1681
- 1682 **138.** Follansbee WP, Curtiss EI, Medsger Jr TA, et al. Physiologic abnormalities of cardiac  
1683 function in progressive systemic sclerosis with diffuse scleroderma. *N Engl J Med*  
1684 1984;310:142–8.  
1685
- 1686 **139.** Lancellotti P, Nkomo VT, Badano LP, Bergler-Klein J, Bogaert J, Davin L, et al. Expert  
1687 consensus for multi-modality imaging evaluation of cardiovascular complications of

- 1688 radiotherapy in adults: a report from the European Association of Cardiovascular Imaging  
1689 and the American Society of Echocardiography. *Eur Heart J Cardiovasc Imaging*.  
1690 2013;**14**:721-40.  
1691
- 1692 **140.** Messroghli D, Nordmeyer S, Dietrich T, Dirsch O, Kaschina E, Savvatis K, et al.  
1693 Assessment of diffuse myocardial fibrosis in rats using small-animal Look-Locker inversion  
1694 recovery T1 mapping. *Circ Cardiovasc Imaging*. 2011;**4**:636-640.  
1695
- 1696 **141.** Constine L, Schwartz R, Savage D, King V, Muhs A. Cardiac function, perfusion, and  
1697 morbidity in irradiated long-term survivors of Hodgkin's disease. *Int J Radiat Oncol Biol Phys*.  
1698 1997;**39**:897-906.  
1699
- 1700 **142.** Marks L, Yu X, Prosnitz R, Zhou SM, Hardenbergh P, Blazing M, et al. The incidence  
1701 and functional consequences of RT-associated cardiac perfusion defects. *Int J Radiat Oncol*  
1702 *Biol Phys*. 2005;**63**:214-223  
1703
- 1704 **143.** Plana JC, Galderisi M, Barac A, Ewer MS, Ky B, Scherrer-Crosbie M, et al. Expert  
1705 consensus for multimodality imaging evaluation of adult patients during and after cancer  
1706 therapy: a report from the American Society of Echocardiography and the European  
1707 Association of Cardiovascular Imaging. *Eur Heart J Cardiovasc Imaging*. 2014;**15**:1063-1093.  
1708
- 1709 **144.** Dato I. How to recognize endomyocardial fibrosis? *J Cardiovasc Med*. 2015 ;**16**:547-  
1710 51.  
1711
- 1712 **145.** Mocumbi AO. Endomyocardial fibrosis: A form of endemic restrictive cardiomyopathy.  
1713 *Glob Cardiol Sci Pract*. 2012 ;**2012**:11  
1714
- 1715 **146.** Bukhman G, Ziegler J, Parry E. Endomyocardial fibrosis: still a mystery after 60 years.  
1716 *PLoS Negl Trop Dis*. 2008;**2**:e97  
1717
- 1718 **147.** Mocumbi AO, Carrilho C, Sarathchandra P, Ferreira MB, Yacoub M, Burke M.  
1719 Echocardiography accurately assesses the pathological abnormalities of chronic  
1720 endomyocardial fibrosis. *Int J Cardiovasc Imaging*. 2011 ; **27**:955-64.  
1721
- 1722 **148.** Mocumbi AO, Ferreira MB, Sidi D, Yacoub MH. A population study of endomyocardial  
1723 fibrosis in a rural area of Mozambique. *N Engl J Med*. 2008;**359**:43-9.  
1724
- 1725 **149.** Kharabish A, Haroun D1. Cardiac MRI findings of endomyocardial fibrosis (Loeffler's  
1726 endocarditis) in a patient with rheumatoid arthritis. *J Saudi Heart Assoc*. 2015;**27**:127-31

- 1727
- 1728 **150.** Schneeweis C, Berger A, Kelle S, Fleck E, Gebker R. Endomyocardial fibrosis in  
1729 patients with confirmed Churg\_Strauss syndrome. *Rheumatology* 2014;53:84.
- 1730
- 1731 **151.** Maia CP, Gali LG, Schmidt A, de Almeida Filho OC, Santos MK, et al. A Challenging  
1732 Differential Diagnosis: Distinguishing between Endomyocardial Fibrosis and Apical  
1733 Hypertrophic Cardiomyopathy. *Echocardiography*. 2016;33:1080-4
- 1734
- 1735 **152.** Cury R, Abbara S, Sandoval LJ, Houser S, Brady T and Palacios IF. Visualization of  
1736 Endomyocardial Fibrosis by Delayed-Enhancement Magnetic Resonance. *Imaging*  
1737 *Circulation*. 2005;111:9, e115-117.
- 1738
- 1739 **153.** Salemi VMC, Rochitte CE, Shiozaki AA, Andrade JM, Parga JR, de A' Vila LF, et al.  
1740 Late gadolinium enhancement magnetic resonance imaging in the diagnosis and prognosis of  
1741 endomyocardial fibrosis patients. *Circ Cardiovasc Imaging*. 2011;4:304-311.
- 1742
- 1743 **154.** Roper D, Hillier SD, Burstow DJ, Platts D. Non-tropical endomyocardial fibrosis  
1744 associated with sarcoidosis. *Eur Heart J Cardiovasc Imaging*. 2014;15:472.
- 1745
- 1746 **155.** Seguela PE, Iriart X, Acar P, Montaudon M, Roudaut R, Thambo JB. Eosinophilic  
1747 cardiac disease : molecular, clinical and imaging aspects. *Arch Cardiovasc Dis* 2015 ; 108 :  
1748 258-68
- 1749
- 1750 **156.** Al Ali AM, Straatman LP, Allard MF, Ignaszewski AP. Eosinophilic myocarditis: case  
1751 series and review of literature. *Can J Cardiol*. 2006;22:1233-7
- 1752
- 1753 **157.** Ommen SR, Seward JB, Tajik AJ. Clinical and echocardiographic features of  
1754 hypereosinophilic syndromes. *Am J Cardiol* 2000 ; 1 : 110-113
- 1755
- 1756 **158.** Simonnet B, Jacquier A, Salaun E, Hubert S, Habib G. Cardiac involvement in  
1757 hypereosinophilic syndrome: role of multimodality imaging. *Eur Heart J Cardiovasc Imaging*.  
1758 2015;16:228
- 1759
- 1760 **159.** Acquatella H, Schiller NB, Puigbó JJ, Gómez-Mancebo JR, Suarez C, Acquatella G.  
1761 Value of two-dimensional echocardiography in endomyocardial disease with and without  
1762 eosinophilia. A clinical and pathologic study. *Circulation*. 1983;67:1219-26.
- 1763

- 1764 **160.** Rotoli B, Catalano L, Galderisi M, Luciano L, Pollio G, Guerriero A, et al. Rapid  
1765 reversion of Loeffler's endocarditis by imatinib in early stage clonal hypereosinophilic  
1766 syndrome. *Leuk Lymphoma*. 2004 ;45:2503-7  
1767
- 1768 **161.** Puvaneswary M, Joshua F, Ratnarajah S. Idiopathic hypereosinophilic syndrome:  
1769 magnetic resonance imaging findings in endomyocardial fibrosis. *Australas Radiol*  
1770 2001;45:524e527.  
1771
- 1772 **162.** Porto AG, McAlindon E, Hamilton M, Manghat N, Bucciarelli-Ducci C. Diagnosing  
1773 cardiac involvement in the hypereosinophilic syndrome by cardiac magnetic resonance.. *Am*  
1774 *J Cardiol*. 2013 Jul 1;112(1):135-6  
1775
- 1776 **163.** Pillar N, Halkin A, Aviram G. Hypereosinophilic syndrome with cardiac involvement:  
1777 early diagnosis by cardiac magnetic resonance imaging. *Can J Cardiol* 2012;515:e11ee13.  
1778
- 1779 **164.** ten Oever J, Theunissen LJ, Tick LW, Verbunt RJ. Cardiac involvement in  
1780 hypereosinophilic syndrome. *Neth J Med*. 2011;69:240  
1781
- 1782 **165.** Haugaa KH, Bergestuen DS, Sahakyan LG, Skulstad H, Aakhus S, Thiis-Evensen E,  
1783 Edvardsen T. Evaluation of right ventricular dysfunction by myocardial strain  
1784 echocardiography in patients with intestinal carcinoid disease. *J Am Soc Echocardiogr*.  
1785 2011;24:644-50.  
1786
- 1787 **166.** Modlin IM, Shapiro MD, Kidd M. Carcinoid tumors and fibrosis: an association with  
1788 no explanation. *Am J Gastroenterol*. 2004;99:2466-78  
1789
- 1790 **167.** Connolly HM, Pellikka PA. Carcinoid heart disease. *Curr Cardiol Rep*. 2006;8:96-101  
1791
- 1792 **168.** Pellikka PA, Tajik AJ, Khandheria BK, Seward JB, Callahan JA, Pitot HC, Kvols LK.  
1793 Carcinoid heart disease. Clinical and echocardiographic spectrum in 74 patients. *Circulation*.  
1794 1993;87:1188-96  
1795
- 1796 **169.** Urheim S, Edvardsen T, Torp H, Angelsen B, Smiseth OA. Myocardial strain by Doppler  
1797 echocardiography. Validation of a new method to quantify regional myocardial function.  
1798 *Circulation*. 2000;102:1158-64  
1799
- 1800 **170.** Zahid W, Bergestuen D, Haugaa KH, Ueland T, Thiis-Evensen E, Aukrust P, Fosse E,  
1801 et al. Myocardial Function by Two-Dimensional Speckle Tracking Echocardiography and

1802 Activin A May Predict Mortality in Patients with Carcinoid Intestinal Disease. *Cardiology*  
1803 2015;132:81-90  
1804

1805 **171.** Moerman VM, Dewilde D, Hermans K. Carcinoid heart disease: typical findings on  
1806 echocardiography and cardiac magnetic resonance. *Acta Cardiol.* 2012 ;67:245-8.  
1807

1808 **172.** Nebigil CG, Etienne N, Messaddeq N, Maroteaux L. Serotonin is a novel survival factor  
1809 of cardiomyocytes: Mitochondria as a target of 5-ht2b receptor signaling. *FASEB J.*  
1810 2003;17:1373-1375  
1811

1812 **173.** Hutcheson JD, Setola V, Roth BL, Merryman WD. Serotonin receptors and heart valve  
1813 disease--it was meant 2b. *Pharmacol Ther.* 2011;132:146-157  
1814

1815 **174.** Fielden MR, Hassani M, Uppal H, Day-Lollini P, Button D, Martin RS, Garrido R, Liu  
1816 X, Kolaja KL. Mechanism of subendocardial cell proliferation in the rat and relevance for  
1817 understanding drug-induced valvular heart disease in humans. *Exp Toxicol Pathol.*  
1818 2010;62:607-613  
1819

1820 **175.** Fowles RE, Cloward TV, Yowell RL. Endocardial fibrosis associated with fenfluramine-  
1821 phentermine. *N Engl J Med.* 1998;338:1316  
1822

1823 **176.** Szymanski C, Marechaux S, Bruneval P, Andrejak M, de Montpréville VT, Belli E, et  
1824 al. Sub obstruction of left outflow tract secondary to benfluorex-induced endocardial fibrosis.  
1825 *IJC Heart Vasculature* 2015;9: 67-69  
1826

1827 **177.** Vaitkus PT, Kussmaul WG. Constrictive pericarditis versus restrictive  
1828 cardiomyopathy: a reappraisal and update of diagnostic criteria. *Am Heart J* 1991;**122**:1431-  
1829 41.  
1830

1831 **178.** Shabetai R. Pathophysiology and differential diagnosis of restrictive cardiomyopathy.  
1832 *Cardiovasc Clin* 1988;**19**:123-32.  
1833

1834 **179.** Kusunose K, Dahiya A, Popović ZB, Motoki H, Alraies MC, Zurick AO, et al.  
1835 Biventricular mechanics in constrictive pericarditis comparison with restrictive  
1836 cardiomyopathy and impact of pericardiectomy. *Circ Cardiovasc Imaging* 2013;**6**:399-406.  
1837

1838 **180.** Francone M, Dymarkowski S, Kalantzi M, Rademakers FE, Bogaert J. Assessment of  
1839 ventricular coupling with real-time cine MRI and its value to differentiate constrictive  
1840 pericarditis from restrictive cardiomyopathy. *Eur Radiol* 2006;**16**:944-51.

- 1841
- 1842 **181.** Welch TD, Ling LH, Espinosa RE, Anavekar NS, Wiste HJ, Lahr BD, et al.
- 1843 Echocardiographic diagnosis of constrictive pericarditis. Mayo clinic criteria. *Circ Cardiovasc*
- 1844 *Imaging* 2014 ; 7 526-34
- 1845
- 1846 **182.** Ha JW, Ommen SR, Tajik AJ, Barnes ME, Ammash NM, Gertz MA, et al. Differentiation
- 1847 of constrictive pericarditis from restrictive cardiomyopathy using mitral annular velocity by
- 1848 tissue Doppler echocardiography. *Am J Cardiol* 2004;**94**:316-9.
- 1849
- 1850 **183.** Ha JW, Oh JK, Ommen SR, Ling LH, Tajik AJ. Diagnostic value of mitral annular
- 1851 velocity for constrictive pericarditis in the absence of respiratory variation in mitral inflow
- 1852 velocity. *J Am Soc Echocardiogr* 2002;**15**:1468-71.
- 1853
- 1854 **184.** Sengupta PP, Mohan JC, Mehta V, Arora R, Pandian NG, Khandheria BK. Accuracy
- 1855 and pitfalls of early diastolic motion of the mitral annulus for diagnosing constrictive
- 1856 pericarditis by tissue Doppler imaging. *Am J Cardiol* 2004;**93**:886-90.
- 1857
- 1858 **185.** Rajagopalan N, Garcia MJ, Rodriguez L, Murray RD, Apperson-Hansen C, Stugaard
- 1859 M, et al. Comparison of new Doppler echocardiographic methods to differentiate constrictive
- 1860 pericardial heart disease and restrictive cardiomyopathy. *Am J Cardiol* 2001;**87**:86-94.
- 1861
- 1862 **186.** Amaki M, Savino J, Ain DL, Sanz J, Pedrizzetti G, Kulkarni H, et al. Diagnostic
- 1863 concordance of echocardiography and cardiac magnetic resonance-based tissue tracking for
- 1864 differentiating constrictive pericarditis from restrictive cardiomyopathy. *Circ Cardiovasc*
- 1865 *Imaging* 2014;**7**:819-27.
- 1866
- 1867 **187.** Adler Y, Charron P, Imazio M, Badano L, Baron-Esquivias G, Bogaert J, et al. 2015
- 1868 ESC Guidelines for the diagnosis and management of pericardial diseases: The Task Force for
- 1869 the Diagnosis and Management of Pericardial Diseases of the European Society of Cardiology
- 1870 (ESC)Endorsed by: The European Association for Cardio-Thoracic Surgery (EACTS). *Eur*
- 1871 *Heart J* 2015;**36**:2921-64.
- 1872
- 1873 **188.** Talreja DR, Edwards WD, Danielson GK, Schaff HV, Tajik AJ, Tazelaar HD, Breen JF,
- 1874 Oh JK. Constrictive pericarditis in 26 patients with histologically normal pericardial
- 1875 thickness. *Circulation* 2003;**108**:1852-7.
- 1876
- 1877 **189.** Yared K, Baggish AL, Picard MH, Hoffmann U, Hung J. Multimodality imaging of
- 1878 pericardial diseases. *JACC Cardiovasc Imaging* 2010;**3**:650-60..
- 1879

- 1880 **190.** Elliott PM, Anastasakis A, Borger MA, Borggrefe M, Cecchi F, Charron P, et al. 2014  
1881 ESC Guidelines on diagnosis and management of hypertrophic cardiomyopathy: the Task  
1882 Force for the Diagnosis and Management of Hypertrophic Cardiomyopathy of the European  
1883 Society of Cardiology. *Eur Heart J.* 2014 ;35:2733-792  
1884
- 1885 **191.** Olivotto I, Maron BJ, Appelbaum E, Harrigan CJ, Salton C, Gibson CM, et al. Spectrum  
1886 and clinical significance of systolic function and myocardial fibrosis assessed by  
1887 cardiovascular magnetic resonance in hypertrophic cardiomyopathy. *Am J Cardiol.*  
1888 2010;106:261-7  
1889
- 1890 **192.** Biagini E, Spirito P, Rocchi G, Ferlito M, Rosmini S, Lai F, et al. Prognostic implications  
1891 of the Doppler restrictive filling pattern in hypertrophic cardiomyopathy. *Am J Cardiol*  
1892 ;104:1727-31.  
1893
- 1894 **193.** Melacini P, Basso C, Angelini A, Calore C, Bobbo F, Tokajuk B, et al.  
1895 Clinicopathological profiles of progressive heart failure in hypertrophic cardiomyopathy. *Eur*  
1896 *Heart J.* 2010;31:2111-23.  
1897
- 1898 **194.** Nistri S, Olivotto I, Betocchi S, Losi MA, Valsecchi G, Pinamonti B, et al. Prognostic  
1899 significance of left atrial size in patients with hypertrophic cardiomyopathy (from the Italian  
1900 Registry for Hypertrophic Cardiomyopathy). *Am J Cardiol.* 2006 ;98:960-5.  
1901
- 1902 **195.** Maron BJ, Spirito P. Implications of left ventricular remodeling in hypertrophic  
1903 cardiomyopathy. *Am J Cardiol.* 1998;81:1339-448  
1904
- 1905 **196.** Olivotto I, Cecchi F, Poggesi C, Yacoub MH.. Patterns of disease progression in  
1906 hypertrophic cardiomyopathy: an individualized approach to clinical staging. *Circ Heart Fail*  
1907 2012;5:535-46  
1908
- 1909 **197.** Habib G, Charron P, Eicher JC, Giorgi R, Donal E, Laperche T, et al; Working Groups  
1910 'Heart Failure and Cardiomyopathies' and 'Echocardiography' of the French Society of  
1911 Cardiology. Isolated left ventricular non-compaction in adults: clinical and echocardiographic  
1912 features in 105 patients. Results from a French registry. *Eur J Heart Fail.* 2011;13:177-85  
1913
- 1914 **198.** Rapezzi C, Leone O, Ferlito M, Biagini E, Cocco F, Arpesella G. Isolated ventricular  
1915 non-compaction with restrictive cardiomyopathy. *Eur Heart J.* 2006 ;27:1927  
1916